

## 5-HT<sub>1A</sub>- versus D<sub>2</sub>-Receptor Selectivity of Flesinoxan and Analogous N<sup>4</sup>-Substituted N<sup>1</sup>-Arylpiperazines

Wilma Kuipers,<sup>\*,†</sup> Chris G. Kruse,<sup>†</sup> Ineke van Wijngaarden,<sup>†</sup> Piet J. Standaar,<sup>†</sup> Martin Th. M. Tulp,<sup>‡</sup> Nora Veldman,<sup>§</sup> Anthony L. Spek,<sup>§,⊥</sup> and Adriaan P. IJzerman<sup>∇</sup>

Departments of Medicinal Chemistry and CNS Pharmacology, Solvay Pharmaceuticals Research Laboratories, P.O. Box 900, 1380 DA Weesp, The Netherlands, Bijvoet Center for Biomolecular Research, Laboratory of Crystal and Structural Chemistry, Utrecht University, Padualaan 8, 3584 CH Utrecht, The Netherlands, and Division of Medicinal Chemistry, Leiden/Amsterdam Center for Drug Research, P.O. Box 9502, 2300 RA Leiden, The Netherlands

Received July 8, 1996<sup>®</sup>

We investigated the structural requirements for high 5-HT<sub>1A</sub> affinity of the agonist flesinoxan and its selectivity versus D<sub>2</sub> receptors. For this purpose a series of arylpiperazine congeners of flesinoxan were synthesized and evaluated for their ability to displace [<sup>3</sup>H]-8-OH-DPAT and [<sup>3</sup>H]spiperone from their specific binding sites in rat frontal cortex homogenates and rat striatum, respectively. Variations were made in the N<sup>4</sup>-substituent and the arylpiperazine region. Effects of N<sup>4</sup>-substitution in the investigated compounds appeared to be quite similar for 5-HT<sub>1A</sub>- and D<sub>2</sub>-receptor affinity. Lipophilicity at a distance of four carbon atoms from the piperazine N<sup>4</sup> atom seems to be the main contributing factor to affinity for both receptors. Our data show that the amide group in the flesinoxan N<sup>4</sup>-substituent is unlikely to interact with the 5-HT<sub>1A</sub> receptor but, instead, acts as a spacer. In contrast to the structure–affinity relationships (SARs) of the N<sup>4</sup>-substituents, selectivity for 5-HT<sub>1A</sub> versus D<sub>2</sub> receptors was gained by the arylpiperazine substitution pattern of flesinoxan. Restriction of flexibility of the N<sup>4</sup>-(benzoylamino)ethyl substituent and its effect on 5-HT<sub>1A</sub>-receptor affinity and activity were also studied. Our data show that in the bioactive conformation, the N<sup>4</sup>-[(*p*-fluorobenzoyl)amino]ethyl substituent is probably directed *anti*-periplanar relative to the H<sub>N4</sub> atom. These results were used to dock flesinoxan (**1**) and two of its congeners (**27** and **33**) into a model of the 5-HT<sub>1A</sub> receptor that we previously reported. Amino acid residues surrounding the N<sup>4</sup>-[(*p*-fluorobenzoyl)amino]ethyl substituent of flesinoxan and its congeners are also present in D<sub>2</sub> receptors. In contrast, several residues that contact the benzodioxane moiety differ from those in D<sub>2</sub> receptors. These observations from the 3D model agree with the 5-HT<sub>1A</sub> SAR data and probably account for the selectivity of flesinoxan versus D<sub>2</sub> receptors.

### Introduction

The family of receptors that are activated by the neurotransmitter serotonin (5-hydroxytryptamine, 5-HT) consists of at least seven types, *i.e.*, 5-HT<sub>1–7</sub> (for recent reviews, see Saudou and Hen<sup>1</sup> and Peroutka<sup>2</sup>). Some of these types have been further subdivided. The 5-HT<sub>1</sub> class contains 5-HT<sub>1A</sub>, 5-HT<sub>1B/1Dβ</sub>, 5-HT<sub>1Dα</sub>, 5-HT<sub>1E</sub>, and 5-HT<sub>1F</sub>, as well as the *Drosophila* 5-HT<sub>dro2A</sub> and 5-HT<sub>dro2B</sub> receptors.<sup>1</sup> The early discovery of 8-OH-DPAT, the *R*-enantiomer of which being a highly selective and potent 5-HT<sub>1A</sub> agonist,<sup>3</sup> enabled the search for new selective compounds for the 5-HT<sub>1A</sub> subtype. This research has led to the discovery of several agonists (flesinoxan, **1**), partial agonists (buspirone, **2**; ipsapirone, **3**; BMY 7378, **4**), and, recently, antagonists ((*S*)-UH-301, **5**; (*S*)-WAY-100135, **6**) at 5-HT<sub>1A</sub> receptors (see Chart 1).<sup>4–7</sup> Flesinoxan (**1**) is selective for 5-HT<sub>1A</sub> receptors. In contrast, considerable affinity for dopamine D<sub>2</sub> receptors was reported<sup>8</sup> for many other N<sup>4</sup>-substituted 5-HT<sub>1A</sub> arylpiperazines.

In this study we investigated the structure–affinity relationships (SARs) of **1** in order to gain insight in the structural parameters determining its high affinity for 5-HT<sub>1A</sub> receptors and selectivity versus D<sub>2</sub> receptors. For this purpose, we synthesized three series of congeners of **1** (sets A–C, structural variation is depicted in Chart 2). 5-HT<sub>1A</sub>- and D<sub>2</sub>-receptor affinities of these compounds were determined in radioligand binding studies. A substantial contribution of log *P* to 5-HT<sub>1A</sub>-receptor affinity has previously been reported for certain N<sup>4</sup>-substituents but not for the arylpiperazine part of the molecule.<sup>9,10</sup> Therefore, we experimentally determined log *P* values of our compounds and investigated a possible correlation with 5-HT<sub>1A</sub>- and D<sub>2</sub>-receptor affinities. As only the series A and B contain variations in the N<sup>4</sup>-substituent, the log *P* evaluation was limited to these compounds (see also Chart 2).

We subsequently investigated the bioactive conformation of the 5-HT<sub>1A</sub>-receptor agonist **1** that was required for docking in our model for the 5-HT<sub>1A</sub> receptor.<sup>11,12</sup> Compound **1** is rather flexible, since it contains several freely rotatable bonds. Therefore, the more rigid compound **33** was chosen as a model compound to study the bioactive conformation of this type of 5-HT<sub>1A</sub>-receptor agonist. The receptor model has previously been shown to rationalize 5-HT<sub>1A</sub> SARs of N<sup>4</sup>-unsubstituted arylpiperazines,<sup>11</sup> as well as affinity and selectivity of several other agonist classes such as tryptamines and aminote-

\* To whom correspondence should be addressed, at the following: tel, 31-2944-79875; fax, 31-2944-80688; e-mail, kuipers-solvay@e-mail.com (or W.Kuipers@duphar.nl).

<sup>†</sup> Department of Medicinal Chemistry.

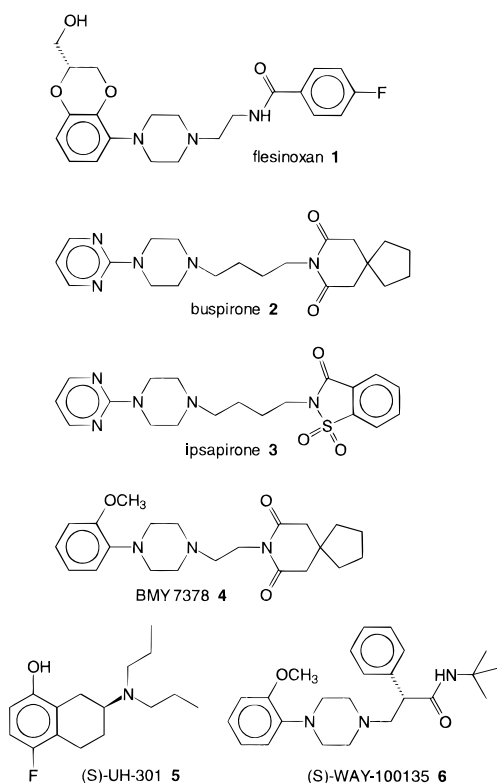
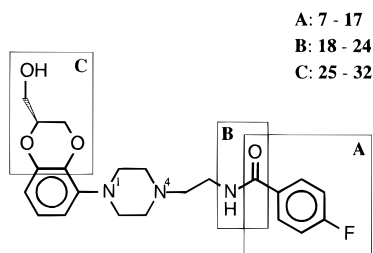
<sup>‡</sup> Department of CNS Pharmacology.

<sup>§</sup> Utrecht University.

<sup>∇</sup> Leiden/Amsterdam Center for Drug Research.

<sup>⊥</sup> Address correspondence pertaining to crystallographic studies to this author.

<sup>®</sup> Abstract published in *Advance ACS Abstracts*, November 15, 1996.

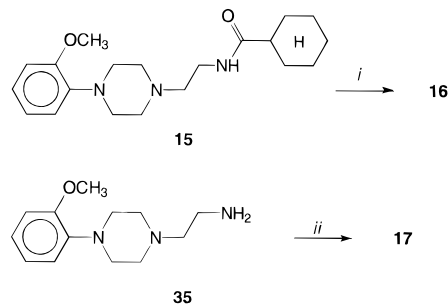
**Chart 1.** Structures of Several 5-HT<sub>1A</sub>-Receptor Ligands**Chart 2.** Variations in the Flesinoxan Structure That Were Investigated in This Study

tralins, and (aryloxy)propanolamine antagonists.<sup>12</sup> It was also shown that agonists and antagonists may occupy very different binding sites at the receptor. A 5-HT<sub>1A</sub> agonistic profile of the compounds **27** and **33** would support the hypothesis that they address the same binding site at the receptor as the full agonist flesinoxan (**1**). Therefore, we studied the 5-HT<sub>1A</sub> functional behavior of the two flexinoxan congeners **27** and **33** prior to the docking studies. The conclusions from the modeling experiments concerning the 3D structure of **33** were supported by the crystal structure determination of this compound.

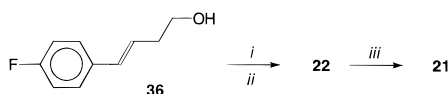
**Chemistry**

The preparation of a number of target compounds (Tables 1–4) has already been described in the literature. The unknown *N*-2-(acylamino)ethyl-substituted (2-methoxyphenyl)piperazines **7**, **9**, **10**, and **12–14** were prepared by acylation of the known *N*-2-aminoethyl precursor **35**,<sup>29</sup> using either the anhydride (for **7**), the acyl chloride (for **9**, **10**, and **13**), or the Mukayama ester (for **12** and **14**) of the corresponding acids.

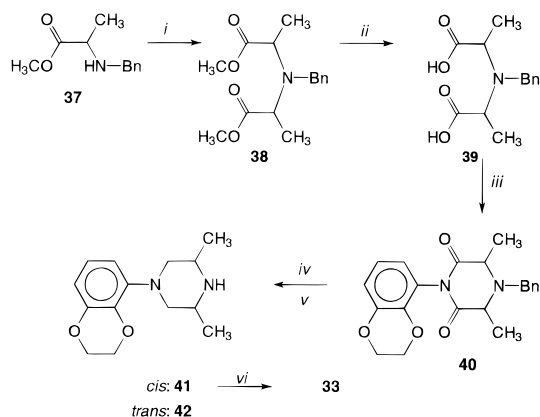
The route of preparation for the amide isomers **16** and **17** is depicted in Scheme 1. The thioamide **16** was

**Scheme 1<sup>a</sup>**

<sup>a</sup> (i) P<sub>2</sub>S<sub>5</sub>, Et<sub>3</sub>N (4 equiv), CH<sub>2</sub>Cl<sub>2</sub>, 20 °C; (ii) C<sub>6</sub>H<sub>11</sub>C(OEt)NH·HCl, EtOH, 20 °C.

**Scheme 2<sup>a</sup>**

<sup>a</sup> (i) MeSO<sub>2</sub>Cl, Et<sub>3</sub>N, CH<sub>2</sub>Cl<sub>2</sub>, 20 °C; (ii) *N*-(2-methoxyphenyl)piperazine, Et(*i*-Pr)<sub>2</sub>N, CH<sub>3</sub>CN, 60 °C; (iii) H<sub>2</sub>, Pd/C, EtOH, 20 °C.

**Scheme 3<sup>a</sup>**

<sup>a</sup> (i) TfOCH(CH<sub>3</sub>)CO<sub>2</sub>Me, Et(*i*-Pr)<sub>2</sub>N, 90 °C, *n*-pentane; (ii) KOH (3 equiv), H<sub>2</sub>O–MeOH followed by aqueous HCl (excess); (iii) CDI (2 × 1.0 equiv), 5-aminobenzo-1,4-dioxane, THF, reflux; (iv) H<sub>2</sub>, Pd/C, EtOAc/MeOH; (v) BH<sub>3</sub>·Me<sub>2</sub>S (2.6 equiv), THF, reflux; then 6 N HCl (excess); (vi) *N*-(4-fluorobenzoyl)aziridine, 80 °C.

conveniently prepared by P<sub>2</sub>S<sub>5</sub> treatment of the corresponding amide **15** in dichloromethane in the presence of an excess of triethylamine at room temperature. The cyclohexylamine **17** resulted from reaction of **35** with the corresponding iminoethyl ether hydrochloride salt in ethanol at room temperature.

The route to compounds **21** and **22** is depicted in Scheme 2. *trans*-4-(4-Fluorophenyl)-3-butenol (**36**) was treated with methanesulfonyl chloride and triethylamine in dichloromethane at 20 °C overnight. The resulting mesylate was subsequently reacted with *N*-(2-methoxyphenyl)piperazine and diisopropylethylamine in acetonitrile at 60 °C overnight. Finally, product **22** could be conveniently hydrogenated with Pd/C as the catalyst in ethanol at 20 °C, giving **21**.

The *cis*-dimethyl-substituted arylpiperazine **33** was synthesized by a stepwise procedure as shown in Scheme 3. *N*-Benzyl-D-alanine methyl ester (**37**) was alkylated with the triflate of racemic methyl lactate<sup>13</sup> to obtain the imino diester **38** as a diastereoisomeric mixture of the *meso* and the *d,l* forms. After converting this mixture into the corresponding imino diacid **39** by saponification, the arylpiperazine moiety was con-

5-HT <sub>1A</sub> D <sub>2</sub>	38 36	I T S L L L G T L I F C A V L G N A C V V A A Y Y A M L L T L L I F I I V F G N V L V C M A	I
5-HT <sub>1A</sub> D <sub>2</sub>	74 72	L I G S L A V T D L M V S V L V L P M A A L Y L I V S L A V A D L L V A T L V M P W V V Y L	II
5-HT <sub>1A</sub> D <sub>2</sub>	109 107	C D L F I A L D V L C C T S S I L H L C A I C D I F V T L D V M M C T A S I L N L C A I	III
5-HT <sub>1A</sub> D <sub>2</sub>	153 152	A A A L I S L T W L I G F L I S I P P M L V T V M I A I V W V L S F T I S C P L L F	IV
5-HT <sub>1A</sub> D <sub>2</sub>	195 189	Y T I Y S T F G A F Y I P L L I M L V L Y F V V Y S S I V S F Y V P F I V T L L V Y	V
5-HT <sub>1A</sub> D <sub>2</sub>	347 376	L G I I M G T F I L C W L P F F I V A L V L P F L A I V L G V F I I C W L P F F I T H I L N I H	VI
5-HT <sub>1A</sub> D <sub>2</sub>	381 408	L G A I I N W L G Y S N S L L N P V I Y A Y F N L Y S A F T W L G Y V N S A V N P I I Y T F N	VII

**Figure 1.** Sequences of the putative transmembrane domains of the rat 5-HT<sub>1A</sub> receptor, which were used for construction of the receptor model, and the corresponding alignment with the rat D<sub>2</sub>-receptor sequence.<sup>12,48</sup> Residues marked boldface were found to be part of the binding site (residues within a sphere of 4 Å) of flesinoxan (**1**), **27**, and **33** in the 5-HT<sub>1A</sub>-receptor model. Residues in the D<sub>2</sub> receptor sequence that differ from those in the modeled binding site are printed in italics. Residues in the D<sub>2</sub> sequence that correspond with those in the modeled 5-HT<sub>1A</sub>-receptor binding site are underlined.

structed by *N,N*-carbonyldiimidazole-promoted coupling with 5-aminobenzo-1,4-dioxane.<sup>14</sup> The imide **40** was converted into the dimethyl-substituted arylpiperazines **41** and **42** by two successive reduction steps (debenzylation and deoxygenation).<sup>14</sup> After these steps the diastereomers **41** and **42** were separated, and the achiral *cis*-diastereomer **41** was subsequently converted into **33** by treatment with *N*-(4-fluorobenzoyl)aziridine.

## Biochemistry

Affinity values of compounds **7–32** were measured as their ability to displace [<sup>3</sup>H]-8-OH-DPAT from central 5-HT<sub>1A</sub> recognition sites in rat frontal cortex and [<sup>3</sup>H]-spiperone from D<sub>2</sub> recognition sites in rat striatum. In addition, 5-HT<sub>1A</sub> agonist activity of compounds **27** and **33** was measured as their potency to inhibit forskolin-stimulated accumulation of intracellular cAMP in cells expressing human 5-HT<sub>1A</sub> receptors.

## Modeling

**Flesinoxan in the 5-HT<sub>1A</sub>-Receptor Model.** Flesinoxan (**1**) was docked into a 5-HT<sub>1A</sub>-receptor model<sup>12</sup> in order to rationalize its high 5-HT<sub>1A</sub> affinity and its selectivity versus D<sub>2</sub> receptors. Two of its congeners (*i.e.*, **27** and **33**) were also incorporated in the docking study. The 5-HT<sub>1A</sub>-receptor model, which was built on the structure of bacteriorhodopsin as a template, was previously shown to explain affinities of *N*<sup>4</sup>-unsubstituted arylpiperazines.<sup>11,12</sup> It consists of seven putative  $\alpha$ -helical transmembrane domains. Sequences of the putative transmembrane domains are shown in Figure 1.<sup>12</sup> For docking procedures possible bioactive conformations were generated, and a putative binding site of **1** in the model was identified. Conformational aspects that were investigated in this study are depicted in Figure 2. For clarity, we use the numbering scheme from Figure 2 throughout the entire paper.

**Binding Site of Phenylpiperazine 5-HT<sub>1A</sub>-Receptor Agonists in the Receptor Model.** Flesinoxan (**1**) is a full 5-HT<sub>1A</sub>-receptor agonist. It is likely, therefore, that its binding site at the 5-HT<sub>1A</sub> receptor overlaps that of other 5-HT<sub>1A</sub> agonists. Binding sites of these other agonists, such as 5-HT and 8-OH-DPAT as well as several arylpiperazine compounds, have been hypoth-

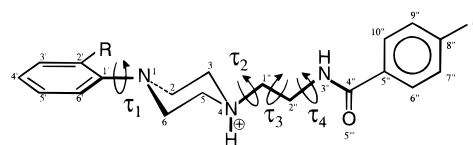


**Figure 2.** Definition of the torsion angles  $\tau_1$  (C6'-C1'-N1-C6), which determines the angle between the benzene and piperazine rings,  $\tau_2$  (H<sub>N4</sub>-N4-C1'-C2'), which primarily determines the direction of the *N*<sup>4</sup>-substituent,  $\tau_3$  (N4-C1''-C2''-N3''), and  $\tau_4$  (C1''-C2''-N3''-C4'').

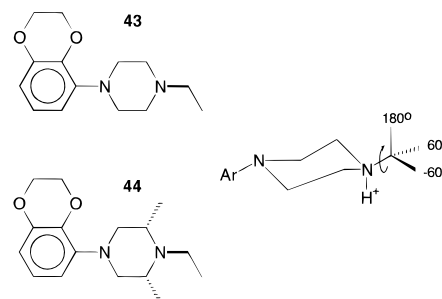


**Figure 3.** Model compounds **43** and **44** that were used for the study of the torsion angle  $\tau_2$  of compounds **27** and **33**, respectively, with MOPAC/AM1 calculations. The three staggered conformations of the C2'' atom with respect to the H<sub>N4</sub> atom with theoretical  $\tau_2$  values of  $-60^\circ$ ,  $60^\circ$ , and  $180^\circ$  are found as energy minima for **43**. The first two *gauche* conformations are not accessible to compound **44**, caused by steric hindrance with the methyl substituents at the piperazine ring. Compounds **43** and **44** share the *anti*-periplanar conformation at  $\tau_2 = 180^\circ$  as an energy minimum. This is also the conformation of  $\tau_2$  in the crystal structure of compound **33**, for which **44** serves as a model compound.

esized in earlier docking studies.<sup>11,12</sup> SAR of these agonists could be rationalized with the putative binding sites in the aforementioned 5-HT<sub>1A</sub>-receptor model. We assumed that the binding site of the arylpiperazine moiety of **1** overlaps with that of **30** and **31**: the *N*<sup>4</sup>-unsubstituted analogs of its congeners **26** and **27** (Table 3).<sup>11</sup> Also the conformation of the arylpiperazine moiety was chosen as previously reported for the *N*<sup>4</sup>-unsubstituted compounds **30** and **31**. Similar arrangements were used for the docking of **27** and **33**. The validity of this choice was investigated by comparison of 5-HT<sub>1A</sub> SAR of *N*<sup>4</sup>-substituted arylpiperazines with that of the corresponding *N*<sup>4</sup>-unsubstituted compounds.

**Bioactive Conformation of Phenylpiperazines: *N*<sup>4</sup>-Substituent.** The conformation of the *N*<sup>4</sup>-substituent is primarily determined by the torsion angles  $\tau_2$ ,  $\tau_3$ , and  $\tau_4$  (see Figure 2). The benzamide part is considered to be fairly rigid (the plane angles between the benzene ring and the amide moiety of the AM1-calculated conformations of compound **33** are all in the range  $25\text{--}30^\circ$ , *vide infra*). The 2,6-dimethyl substituents at the piperazine ring in compound **33** restrict the conformational freedom of the *N*<sup>4</sup>-[(*p*-fluorobenzoyl)-amino]ethyl substituent. The effect of the dimethyl substitution in this compound on 5-HT<sub>1A</sub>-receptor affinity and activation was determined.

Also the conformational effects were investigated. For this purpose, firstly the rotational barrier of the *N*<sup>4</sup>-ethyl chain in the hypothetical compounds **43** and **44** (see Figure 3) was studied with semiempirical MOPAC/AM1 calculations. In these compounds, the benzamide moiety of **27** and **33** is replaced by a hydrogen atom, allowing the study of the torsion angle  $\tau_2$  independently

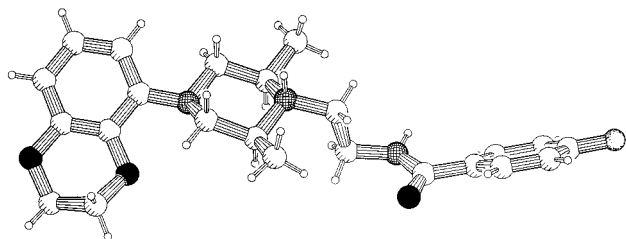


**Figure 4.** PLUTON<sup>49</sup> representation of the conformation of compound **33** in the crystal structure. The torsion angles  $\tau_1$  (C6'-C1'-N1-C6),  $\tau_2$  (HN<sub>4</sub>-N4-C1'-C2'),  $\tau_3$  (N4-C1'-C2'-N3'), and  $\tau_4$  (C1'-C2'-N3'-C4') are  $-11.3^\circ$  (3),  $176.9^\circ$  (3),  $169.7^\circ$  (2), and  $80.0^\circ$  (3), respectively (see also Figure 2). For clarity the fumarate counterion, which is hydrogen bonded to the basic nitrogen N4 atom and the amide NH, is not shown.

from  $\tau_3$  and  $\tau_4$ . Thus **43** and **44** may serve as model compounds for the investigation of  $\tau_2$  of compounds **27** and **33**, respectively. Results of this conformational analysis were supported by the crystal structure of compound **33** (Figure 4). Secondly, possible conformations of the complete *N*<sup>4</sup>-[(*p*-fluorobenzoyl)amino]ethyl chain were generated by varying  $\tau_3$  and  $\tau_4$  in the RANDOMSEARCH option of the SYBYL program, using the crystal structure of compound **33** as the starting geometry (for details, see the Experimental Section). This option locates energy minima by randomly adjusting the chosen torsion angles (here  $\tau_3$  and  $\tau_4$ ) and minimizing the energy of the resulting geometry (see also the Experimental Section). The conformation of the arylpiperazine moiety was constrained during this procedure because the Molecular Mechanics (MM) methods, as used in the RANDOMSEARCH option, are less reliable for calculation of this moiety.<sup>11,15</sup> The unique conformations of **33** that were found were subsequently fully energy-minimized with the semiempirical method MOPAC/AM1,<sup>16</sup> which has been shown to be suitable for arylpiperazine conformational calculations.<sup>15</sup> The resulting conformations (energy  $\leq 3$  kcal/mol above the absolute minimum energy) were checked for their ability to fit the 5-HT<sub>1A</sub>-receptor model and used for further docking studies.

## Results and Discussion

**SARs at 5-HT<sub>1A</sub> and D<sub>2</sub> Receptors: Variations in A (Table 1).** Replacement of the phenyl ring of compound **8** by a methyl group, as in compound **7**, is detrimental for the affinity for 5-HT<sub>1A</sub> and dopamine D<sub>2</sub> receptors. Apparently, the benzene ring in **8** provides an additional interacting group for both receptors. Replacement of the benzene ring of **8** by 2-thiophene as in **9** does not change either the 5-HT<sub>1A</sub>- or D<sub>2</sub>-receptor affinity. In contrast, its replacement by more polar aromatic rings like 2-furan (**10**) and 2-pyrrole (**11**) or polar six-membered rings like 4-pyridyl (**12**) and 2,4-pyrimidyl (**13**) reduces 5-HT<sub>1A</sub>-receptor affinity about 10-fold, while the *m*-pyridine in **14** reduces the receptor affinity more than 2 log units. Similar effects of replacement of the benzene ring of **8** with other aromatic rings were observed for D<sub>2</sub>-receptor affinity, although the polar five-membered rings in **10** and **11** lower affinity less dramatically (approximately 5-fold) than the polar six-membered rings in **12**–**14** (15–44-fold reduction). Thus, apolar aromatic rings are preferred over more polar aromatic rings in this position of the *N*<sup>4</sup>-substituent for both 5-HT<sub>1A</sub> and D<sub>2</sub> receptors.

**Table 1.** 5-HT<sub>1A</sub>- and D<sub>2</sub>-Receptor Affinities of Compounds 7–17 (A)

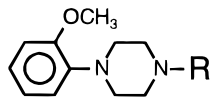
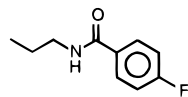
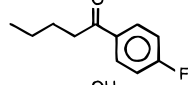
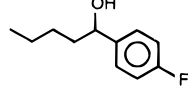
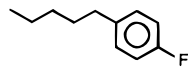
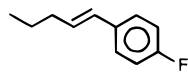
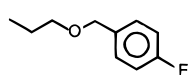
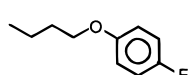
		$K_i \pm \text{SEM}$ (nM) <sup>a</sup>	
R	no.	5-HT <sub>1A</sub>	D <sub>2</sub>
	7	800 ± 70	1100 ± 40
	8	1.3 ± 0.3	13 ± 4
	9	1.6 ± 0.3	17 ± 2
	10	18 ± 4	73 ± 21
	11	16 ± 3	64 ± 4
	12	18 ± 1	230 ± 40
	13	15 ± 4	250 ± 50
	14	140 ± 40	570 ± 190
	15	0.8 ± 0.3	23 ± 6
	16	0.32 ± 0.04	6.4 ± 1.7
	17	4.5 ± 0.9	130 ± 10

<sup>a</sup>  $K_i$  values for the displacement of [<sup>3</sup>H]-8-OH-DPAT from central 5-HT<sub>1A</sub> recognition sites in rat frontal cortex homogenates and of [<sup>3</sup>H]spiperone from D<sub>2</sub> binding sites in rat striatum.  $K_i$  values are based on  $n = 3$  determinations, each using four to six concentrations in triplicate.

Saturation of the benzene ring in **8** to cyclohexane in **15** has little effect on the affinity for both 5-HT<sub>1A</sub> and D<sub>2</sub> receptors. The high affinity of **15** for 5-HT<sub>1A</sub> and D<sub>2</sub> receptors indicates that the lipophilic rather than the aromatic character of the substituent contributes to receptor affinity. Lipophilicity may also play a role in the approximately 3-fold increase in both 5-HT<sub>1A</sub>- and D<sub>2</sub>-receptor affinity by replacement of the benzamide C=O by C=S (compare **16** with **15**). In agreement with this idea, both affinities are reduced approximately 6-fold by replacement of C=O in **15** by C=NH in **17**. Of this series of compounds (A), the cyclohexylthioamide analog **16** is the most potent ligand at both 5-HT<sub>1A</sub> and D<sub>2</sub> receptors.

**Variations in B (Table 2).** In Table 2 variations (B) of the amide moiety of the [(*p*-fluorobenzoyl)amino]-ethyl group are shown. The *p*-fluoro substituent in **18** has no influence on 5-HT<sub>1A</sub>- and slightly increases D<sub>2</sub>-receptor affinity (compare with **8**). Replacement of the amide NH by CH<sub>2</sub> (in **19**) has little influence on 5-HT<sub>1A</sub>-

**Table 2.** 5-HT<sub>1A</sub>- and D<sub>2</sub>-Receptor Affinities of Compounds 18–24 (B)

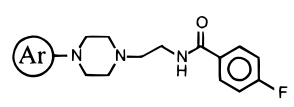
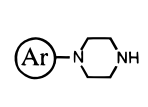
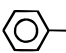
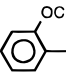
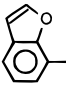
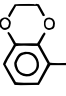
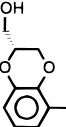
		$K_i \pm \text{SEM (nM)}^a$	
R	no.	5-HT <sub>1A</sub>	D <sub>2</sub>
	18	1.0 ± 0.3	5.0 ± 0.8
	19	1.0 ± 0.2	3.1 ± 0.5
	20	2.5 ± 0.2	3.4 ± 0.6
	21	1.1 ± 0.3	3.3 ± 0.4
	22	1.8 ± 0.2	4.1 ± 1.1
	23	22 ± 5	10 ± 1
	24	3.4 ± 0.7	3.3 ± 0.5

<sup>a</sup>  $K_i$  values for the displacement of [<sup>3</sup>H]-8-OH-DPAT from central 5-HT<sub>1A</sub> recognition sites in rat frontal cortex homogenates and of [<sup>3</sup>H]spiperone from D<sub>2</sub> binding sites in rat striatum.  $K_i$  values are based on  $n = 3$  determinations, each using four to six concentrations in triplicate.

or D<sub>2</sub>-receptor affinity. Reduction of the keto group in **19** to hydroxy in **20**, and even its complete removal as in the (*p*-fluorophenyl)butane analogs **21** and **22**, has only minor effects on affinity for both receptors. The double bond in **22** may be conjugated with the aromatic  $\pi$ -system of the benzene ring in a similar manner as the amide group in **18**. Thus, neither the electrostatic effect of the C=O group nor the conformational effect of the amide function in **18** seem to influence its affinity for 5-HT<sub>1A</sub> and D<sub>2</sub> receptors, respectively. In contrast introduction of an ether oxygen as in **23** reduces affinity for both receptors. Apparently, an electronegative atom at this position is unfavorable. Shifting this oxygen atom by one position toward the benzene ring, like in compound **24**, restores both 5-HT<sub>1A</sub>- and D<sub>2</sub>-receptor affinities to similar values as observed for compounds **18**–**22**. None of the variations of the amide moiety in this series (B) results in selective 5-HT<sub>1A</sub> ligands.

**Variations in C (Table 3).** The results in Table 3 show that compounds with variation in the aryl part (C; see Chart 2) may display larger differences between 5-HT<sub>1A</sub>- and D<sub>2</sub>-receptor affinities than compounds in the former two series (A and B, respectively). Omitting the 2-methoxy group of compound **18**, giving the unsubstituted phenylpiperazine **25**, for instance, enhances the selectivity for 5-HT<sub>1A</sub> receptors by a factor of 4. Apparently, the presence of a 2-methoxy group is more favorable for D<sub>2</sub> than 5-HT<sub>1A</sub> receptors. On the other hand, incorporation of the 2-methoxy group into a furan ring as in **26** is highly favorable for 5-HT<sub>1A</sub>-receptor affinity, whereas the affinity for D<sub>2</sub> receptors is not

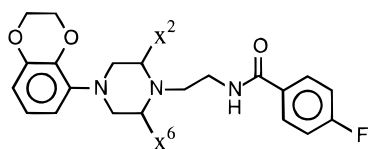
**Table 3.** 5-HT<sub>1A</sub>- and D<sub>2</sub>-Receptor Affinities of Compounds 25–32 (C)

						
$K_i \pm \text{SEM (nM)}^a$				$K_i \pm \text{SEM (nM)}^a$		
Ar	no.	5-HT <sub>1A</sub>	D <sub>2</sub>	no.	5-HT <sub>1A</sub>	D <sub>2</sub>
	25	4.9 ± 1.5	92 ± 17	28	500 ± 20	6800 ± 600
	18	1.0 ± 0.3	5.0 ± 0.8	29	170 ± 20	1200 ± 40
	26	0.15 ± 0.01 <sup>b</sup>	5.3 ± 0.9	30	13 ± 2	780 ± 80
	27	0.30 ± 0.04 <sup>b</sup>	14 ± 1	31	40 ± 5	1100 ± 90
	1	1.7 ± 0.2	140 ± 30	32	59 ± 11	> 10,000

<sup>a</sup>  $K_i$  values for the displacement of [<sup>3</sup>H]-8-OH-DPAT from central 5-HT<sub>1A</sub> recognition sites in rat frontal cortex homogenates and of [<sup>3</sup>H]spiperone from D<sub>2</sub> binding sites in rat striatum.  $K_i$  values are based on  $n = 3$  determinations, each using four to six concentrations in triplicate. <sup>b</sup> 5-HT<sub>1A</sub>-receptor affinity data taken from van Steen *et al.*<sup>18</sup>

affected. The result is a significant increase in selectivity (ratio D<sub>2</sub>/5-HT<sub>1A</sub> is 35.3). Replacement of 2-methoxyphenyl in **18** by benzodioxane yields compound **27** which is slightly less potent than the benzofuran analog **26** but even more selective for 5-HT<sub>1A</sub> when compared to D<sub>2</sub> receptors (ratio D<sub>2</sub>/5-HT<sub>1A</sub> is 46.7). This selectivity is further increased to a factor of 82.4 by substitution of the dioxane ring at the 2-position with a CH<sub>2</sub>OH group as in **1**, which is less favorable for D<sub>2</sub>- than 5-HT<sub>1A</sub>-receptor affinity (compare with **27**). Thus, selectivity of **1** for 5-HT<sub>1A</sub> versus D<sub>2</sub> receptors seems to be largely due to the arylpiperazine aromatic ring system rather than the N<sup>4</sup>-[(*p*-fluorobenzoyl)amino]ethyl substituent.

**5-HT<sub>1A</sub> SARs for Modeling: Analysis of Binding Site and Conformation of N<sup>4</sup>-Substituted Compared to N<sup>4</sup>-Unsubstituted Phenylpiperazines (Table 3).** Table 3 also shows 5-HT<sub>1A</sub> SARs of phenylpiperazines carrying N<sup>4</sup>-[(*p*-fluorobenzoyl)amino]ethyl substituents and those of the corresponding N<sup>4</sup>-unsubstituted compounds. Addition of a 2-methoxy group to **25**, as in **18**, increases 5-HT<sub>1A</sub>-receptor affinity by a factor of 5, while in the corresponding N<sup>4</sup>-unsubstituted compounds **28** and **29**, this increase amounts to a factor of 3. Replacement of the benzene ring of **25** and **28** with benzofuran, yielding **26** and **30**, raises 5-HT<sub>1A</sub>-receptor affinity by factors of 33 and 38, respectively. A similar

**Table 4.** *In Vitro* 5-HT<sub>1A</sub>-Receptor Data of Flesinoxan Congeners **27** and **33**

X <sup>2</sup> , X <sup>6</sup>	no.	K <sub>i</sub> ± SEM (nM) <sup>a</sup>	EC <sub>50</sub> ± SEM (nm) <sup>b</sup>
H, H	<b>27</b>	0.30 ± 0.04	0.90 ± 0.05
<i>cis</i> -dimethyl	<b>33</b>	1.0 ± 0.4	0.78 ± 0.16

<sup>a</sup> K<sub>i</sub> values for the displacement of [<sup>3</sup>H]-8-OH-DPAT from central 5-HT<sub>1A</sub> recognition sites in rat frontal cortex homogenates. K<sub>i</sub> values are based on *n* = 3 determinations, each using four to six concentrations in triplicate. <sup>b</sup> Potency at human 5-HT<sub>1A</sub> receptors in inhibiting forskolin-stimulated accumulation of intracellular cAMP. EC<sub>50</sub> values based on three independent experiments (see also the Experimental Section).

**Table 5.** Measured log *P* Values for Compounds from Tables 1 and 2

compd	measured log <i>P</i> <sup>a</sup>	pK <sub>i</sub> <sup>b</sup>	
		5-HT <sub>1A</sub>	D <sub>2</sub>
<b>7</b>	0.5	6.1	6.0
<b>8</b>	2.2	8.9	7.9
<b>9</b>	2.0	8.8	7.8
<b>10</b>	1.6	7.7	7.1
<b>11</b>	1.6	7.8	7.2
<b>12</b>	ND	7.7	6.6
<b>13</b>	1.5	7.8	6.6
<b>14</b>	1.2	6.8	6.3
<b>15</b>	2.8	9.1	7.9
<b>16</b>	3.7	9.5	8.2
<b>17</b>	3.4	8.3	6.9
<b>18</b>	2.5	9.0	8.3
<b>19</b>	3.6	9.0	8.6
<b>20</b>	3.4	8.6	8.5
<b>21</b>	4.8	9.0	8.5
<b>22</b>	4.7	8.7	8.4
<b>23</b>	3.6	7.7	8.0
<b>24</b>	4.1	8.5	8.5

<sup>a</sup> *n*-Octanol/water coefficients were determined by an HPLC method; ND = not determined. log *P* values below 2.1 were obtained by extrapolation; interpolated values (in the range 2.1–5.7) have a 95% confidence interval of ±0.4. <sup>b</sup> pK<sub>i</sub> (*i.e.*, –log K<sub>i</sub>) values were calculated from the K<sub>i</sub> values (in M) in Tables 2 and 3.

replacement with benzodioxane in **27** and **31** gives 16- and 13-fold increases of 5-HT<sub>1A</sub>-receptor affinity when compared to **25** and **28**. Addition of a CH<sub>2</sub>OH substituent to **27** and the corresponding *N*<sup>4</sup>-unsubstituted compound **31** (eltoprazine) gives compounds **1** and **32**, respectively. This CH<sub>2</sub>OH group slightly lowers 5-HT<sub>1A</sub>-receptor affinity, although the effect for the *N*<sup>4</sup>-unsubstituted compound **32** is less pronounced than for the *N*<sup>4</sup>-substituted compound **1**. Thus, effects of substitution in the aromatic part of the arylpiperazine moiety for the investigated *N*<sup>4</sup>-substituted arylpiperazines and the corresponding *N*<sup>4</sup>-unsubstituted compounds appear to be rather similar. Therefore it seems likely that the arylpiperazine parts of these compounds address similar binding sites at 5-HT<sub>1A</sub> receptors. This hypothesis is corroborated by the fact that both *N*<sup>4</sup>-unsubstituted compounds, **30** and eltoprazine (**31**), as well as *N*<sup>4</sup>-substituted arylpiperazines from this series, **27** and **1**, display agonist properties at 5-HT<sub>1A</sub> receptors (for compound **27**, see Table 4).<sup>4,11</sup>

***In Vitro* 5-HT<sub>1A</sub> Functional Behavior of Flesinoxan Congeners **27** and **33** (Table 4).** Results from

Table 4 show that compound **27**, like **1**, is a potent agonist at 5-HT<sub>1A</sub> receptors, also with full intrinsic activity (data not shown). *cis*-Dimethyl substitution of the piperazine ring yields the similarly potent 5-HT<sub>1A</sub>-receptor agonist **33** (intrinsic activity α = 0.86 ± 0.14). Apparently, the methyl groups do not affect the binding mode of compound **33** at 5-HT<sub>1A</sub> receptors, although these groups dramatically reduce the conformational freedom of its *N*<sup>4</sup>-substituent. Therefore **33** was used as a model compound for the study of the bioactive conformation of **1** and **27**.

**Influence of Lipophilicity of *N*<sup>4</sup>-Substituents on 5-HT<sub>1A</sub>- and D<sub>2</sub>-Receptor Affinity.** Partition coefficients (*n*-octanol/water) of compounds **7–11** and **13–24** were determined by a high-performance liquid chromatographic (HPLC) method. These compounds of series A and B contain varying *N*<sup>4</sup>-substituents. The results (reported as log *P*) are collected in Table 5. The lipophilicity of the substituent attached to the amide moiety appears to greatly influence the affinity of compounds **7–11** and **13–15** for 5-HT<sub>1A</sub> as well as D<sub>2</sub> receptors. The log *P* values of these compounds correlate well with 5-HT<sub>1A</sub>- and D<sub>2</sub>-receptor affinity (correlation coefficients for pK<sub>i</sub> versus log *P* are 0.96 and 0.93, respectively). Also replacement of the polar C=O group in **15** with the more lipophilic C=S in **16** increases both receptor affinities. Compound **17** may be somewhat more hydrophilic than **15** or **16** as a result of (partial) protonation of the imino moiety (see also the <sup>1</sup>H NMR data in the Experimental Section). The given log *P* value represents the uncharged form (see the protocol in the Experimental Section). The more hydrophilic nature of **17** might account for the lower 5-HT<sub>1A</sub>- and D<sub>2</sub>-receptor affinities of this compound when compared to **15** and **16**.

In contrast to the A series, lipophilic dependence of 5-HT<sub>1A</sub>- or D<sub>2</sub>-receptor affinity is completely absent for compounds of series B. Correlation coefficients of log *P* of compounds **18–24** with 5-HT<sub>1A</sub>- and D<sub>2</sub>-receptor affinity values from Table 5 are 0.03 and 0.28, respectively. However, the log *P* values of these compounds are in general higher than those of compounds from series A. Therefore, it may also be argued that the lipophilicity of the entire chain should be sufficiently high for good binding at 5-HT<sub>1A</sub> and D<sub>2</sub> receptors. The observed effects of log *P* for compounds of the A and B series are similar for both 5-HT<sub>1A</sub>- and D<sub>2</sub>-receptor types.

Our results for the 5-HT<sub>1A</sub> receptor are in agreement with previous studies by Mokrosz *et al.*<sup>9</sup> and van Steen *et al.*<sup>10</sup> of arylpiperazines carrying *N*<sup>4</sup>-alkyl substituents. In these studies it was shown that 5-HT<sub>1A</sub>-receptor affinity increases with growing alkyl chain length, mainly in the region C4–C6. These alkyl substituents may partly overlap the -C(=O)-R moiety (R = aryl or cyclohexyl) of our compounds. We found a considerable contribution of lipophilicity to affinity for 5-HT<sub>1A</sub> receptors for this part of the *N*<sup>4</sup>-substituent, which resembles the effect of *N*<sup>4</sup>-alkyl substituents. In addition, our compounds displayed a similar correlation between log *P* and their affinity for D<sub>2</sub> receptors.

van Steen *et al.* previously found that the presence of an amide moiety is not a prerequisite for high 5-HT<sub>1A</sub> affinity.<sup>17</sup> Using CoMFA models, the affinity of *N*<sup>4</sup>-substituents containing an amide moiety could be fully

explained by steric field descriptors. Thus, the hydrogen-bonding capacity of the amide moiety seems to be of minor importance for 5-HT<sub>1A</sub>-receptor affinity. Our experimental data confirm these results and show that the amide moiety merely acts as a spacer instead. In addition we show that the same rule applies to D<sub>2</sub>-receptor affinity as well.

#### Crystal Structure Verification of Compound 33.

The X-ray structure of compound **33** is shown in Figure 4. The observed torsion angle  $\tau_1$  is  $-11.3^\circ$  (3). This is in agreement with previous results concerning the bioactive conformation of *N*<sup>4</sup>-unsubstituted *N*<sup>1</sup>-arylpiperazine agonists at 5-HT<sub>1A</sub> receptors.<sup>11</sup> We found that singly *ortho*-substituted agonists of this class probably bind at 5-HT<sub>1A</sub> receptors in a semicoplanar conformation with torsion angle  $\tau_1 \approx 0^\circ$ . In this conformation, the plane angle between the piperazine and the benzene ring is approximately  $30^\circ$ . Thus, a similar conformation for the arylpiperazine moiety was found in the crystal structure of the (*N*<sup>4</sup>-substituted) potent 5-HT<sub>1A</sub> receptor agonist **33**.

**Modeling: Phenylpiperazines in the 5-HT<sub>1A</sub>-Receptor Model. Bioactive Conformation of Phenylpiperazines. *N*<sup>4</sup>-Substituent Conformation—Calculations.** Figure 5 shows the results of MOPAC/AM1 calculations of  $\tau_2$ , for the hypothetical compounds **43** (a) and **44** (b), respectively (structures in Figure 3). For **43**, three conformations are found as minima, with the C2'' atom staggered relative to the H<sub>N4</sub> atom. The *anti*-periplanar conformation at  $\tau_2 = 180^\circ$  is also found as a minimum for the *cis*-dimethyl analog **44**. The two other minima of **43** (*gauche* conformers) are not accessible to **44** because of severe steric hindrance between the C2'' methyl group and the two equatorially positioned methyl substituents at the piperazine ring. These results are in agreement with the crystal structure of compound **33**, which is in the *anti*-periplanar conformation ( $\tau_2 = 176.9^\circ$  (3); see Figure 4). Although it might be argued that  $\tau_2 = 0^\circ$  is also accessible to both **43** and **44** (not a minimum for **43**, but the energy is within 3 kcal/mol of the absolute minimum energy), it seems less likely to be the bioactive conformation. In this conformation, the *N*<sup>4</sup>-substituent is eclipsed relative to the H<sub>N4</sub> atom and directed toward the putative NH<sup>+</sup>-interacting group at the receptor. Thus, in the  $\tau_2 = 0^\circ$  conformation, the *N*<sup>4</sup>-substituent is likely to bump into essential receptor volume. Therefore, the crystal structure of **33**, with  $\tau_2 = 176.9^\circ$  (3), was used to further study the bioactive conformation.

The RANDOMSEARCH analysis of  $\tau_3$  and  $\tau_4$  yielded 20 conformations with energies (Tripos force field) ranging from 116.7 to 119.2 kcal/mol. Subsequent full energy minimization with MOPAC/AM1 further reduced the number of favorable conformations to eight (A–H; see Table 6). The conformations A and B have  $\tau_3$  values of approximately  $180^\circ$ ; in conformation H  $\tau_3$  amounts to  $-63.8^\circ$ . The torsion angle  $\tau_3$  for the conformations C–G is in the range  $64.0$ – $76.1^\circ$ . Conformations C–G can be divided in two clusters, separated by their  $\tau_4$  values. The torsion angle  $\tau_4$  determines the orientation of the amide moiety (see Figure 6). Cluster 1 is formed by C and D ( $\tau_4$  is  $-104.2^\circ$  and  $-105.9^\circ$ , respectively). In conformations E–G (cluster 2), the direction of the amide moiety is shifted approximately  $180^\circ$ , with  $\tau_4$  values in the range  $65.6$ – $75.5^\circ$ . Within the clusters

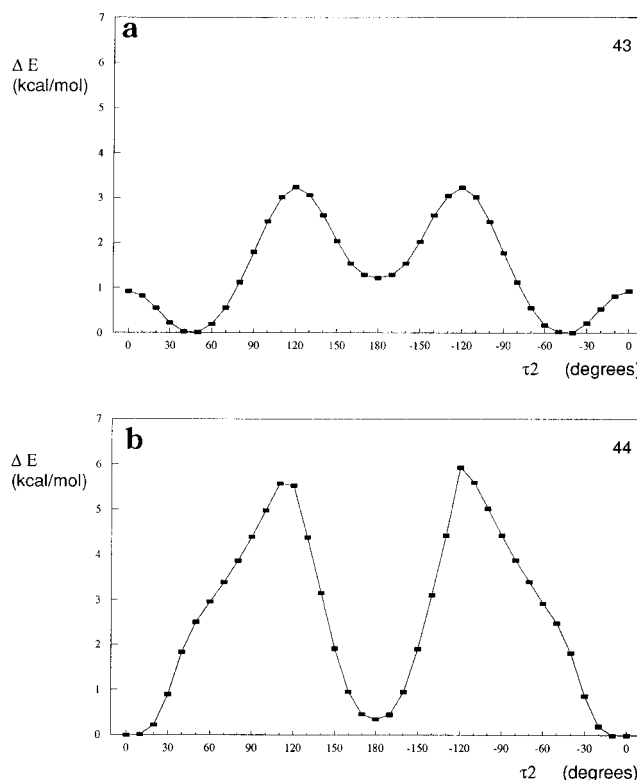


**Figure 5.** Results of MOPAC/AM1 calculations of the torsion angle  $\tau_2$  of compounds **43** (a) and **44** (b), which serve as model compounds for **27** and **33**, respectively. Energy is relative to the calculated absolute minimum. For compound **43** three staggered minimum energy conformations are calculated with  $\tau_2$  values of  $-45^\circ$ ,  $45^\circ$ , and  $180^\circ$ , respectively. In conformations  $-45^\circ$  and  $45^\circ$ , the C2'' atom is positioned *gauche* relative to the H<sub>N4</sub> atom; in the  $180^\circ$  minimum this orientation is *anti*-periplanar. Only the latter conformation is energetically favored by compound **44** also, since in the *gauche* conformations the C2'' atom is severely sterically hindered by the two methyl substituents at the piperazine ring. The second minimum of **44** is the eclipsed conformation at  $\tau_2 = 0^\circ$ , in which the C2'' atom points in the same direction as the H<sub>N4</sub> atom. This is not a minimum energy conformation for compound **43**, although its energy is within 3 kcal/mol of the absolute minimum.

differences occur mainly in the angle between the amide moiety and the benzene ring of the *N*<sup>4</sup>-substituent (*i.e.*, N3''–C4''–C5''–C6''). For C and D this torsion angle amounts to  $153.2^\circ$  and  $-150.9^\circ$ , respectively. For E–G this angle is  $-152.7^\circ$ ,  $154.3^\circ$ , and  $150.5^\circ$ , respectively. Thus, conformations F and G are practically identical.

Structure A closely resembles the crystal structure of **33**. This indicates that our approach indeed yields accessible low-energy conformations. The eight potentially bioactive conformations (A–H) were further investigated for their ability to fit the 5-HT<sub>1A</sub>-receptor model<sup>12</sup> in a docking study.

**Compounds 1, 27, and 33 in the 5-HT<sub>1A</sub>-Receptor Model.** Conformations A, B, and H of compound **33** and the close analogs **1** and **27** (Table 6) could not be accommodated in the 5-HT<sub>1A</sub>-receptor model, as the benzamide part of their *N*<sup>4</sup>-substituents caused severe steric hindrance with the backbones of either helix VI (conformation H) or helix VII (conformations A and B; see Figure 7, top). The complexes of the resulting conformations C–G with the 5-HT<sub>1A</sub>-receptor model were further minimized. These conformations (C–G)

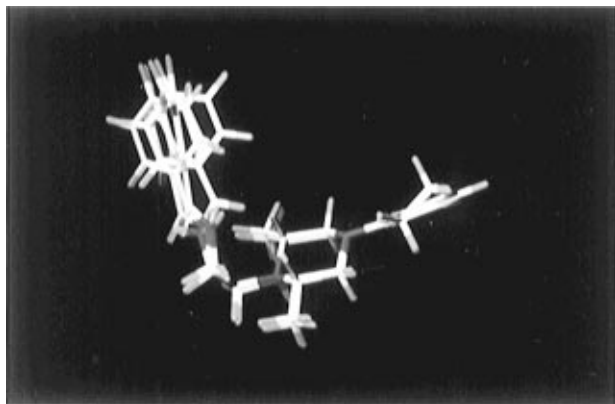


**Figure 6.** Potentially bioactive conformations C and D (cluster 1) and E–G (cluster 2) of compound **33**, resulting from RANDOMSEARCH analysis and subsequent minimization with MOPAC/AM1. The compounds differ in the values for  $\tau_4$ , which determines the direction of the amide group. This torsion angle is approximately  $-105^\circ$  for C and D and varies between  $65.6^\circ$  and  $75.5^\circ$  for E–G. As a result, the C=O group (red) of C and D is pointing to the 'right', while that of conformations E–G is pointing to the 'left' side. Still the *p*-fluorophenyl substituents of both clusters overlap in space. Within the clusters differences occur mainly in the angle between the amide moiety and the benzene ring of the *N*<sup>4</sup>-substituent (*i.e.*, N3''–C4''–C5''–C6''). For C and D this torsion angle amounts to  $153.2^\circ$  and  $-150.9^\circ$ , respectively. For E–G this angle is  $-152.7^\circ$ ,  $154.3^\circ$ , and  $150.5^\circ$ , respectively.

all have  $\tau_3$  values of approximately  $70^\circ$  and consequently occupied a similar region in the 5-HT<sub>1A</sub>-receptor model (see also Figure 6). For **1**, as well as for **27** and **33**, the conformations C and D converged to stable receptor–ligand complexes. For example, Figure 7, bottom, shows **1** in the receptor model in conformation C. The conformations E–G fitted the model slightly worse, due to steric hindrance with the side chain of Trp358 in helix VI. This steric hindrance, or even that of conformations A, B, and H with the helical backbones, does not completely rule out these conformations as potentially bioactive. It is of interest, however, that the surroundings of compounds **1**, **27**, and **33** in conformations C and D after minimization are in good agreement with SAR data. Thus, despite the uncertainty in the exact atomic coordinate positions, which is considered to be the major imperfection of all bacteriorhodopsin-based models of G protein-coupled receptors (GPCRs), our ligand–receptor model accounts for 5-HT<sub>1A</sub> affinity and selectivity versus D<sub>2</sub> receptors (*vide infra*).

For example, a lipophilic pocket is formed by Cys120, Ile124, Leu127, Phe354, Cys357, Trp358, and Phe361 and might account for the considerable contribution of log *P* to both 5-HT<sub>1A</sub>- and D<sub>2</sub>-receptor affinity. This pocket is located in the direction of the C=O group of the *N*<sup>4</sup>-substituent and its benzene ring (see Figure 8, top). The conformations E–G essentially occupy a similar binding region at the 5-HT<sub>1A</sub>-receptor model as conformations C and D (see also Figure 6). Therefore, the residues surrounding the *p*-fluorophenyl moiety of compounds **1**, **27**, and **33** in conformations E–G are similar to those in conformations C and D. However, the C=O group in conformations E–G is directed away from the lipophilic pocket and toward Ser393 at helix VII. Thus, two possible orientations of the amide moiety in the model are found, in which the C=O group of the amide moiety points in the direction of lipophilic con-

formations C and D) or hydrophilic (conformations E–G) residues. This observation from the model may account for the fact that 5-HT<sub>1A</sub>-receptor affinity is hardly affected by the replacement of the polar amide moiety with more lipophilic groups in the compounds of series B.

In the model, the residues that surround the *N*<sup>4</sup>-substituent in the 5-HT<sub>1A</sub>-receptor model (*i.e.*, Asp116, Cys120, Ser123, Ile124, and Leu127, helix III; Phe354, Cys357, Trp358, and Phe361, helix VI; Ser393, helix VII) are also present in D<sub>2</sub> receptors (see Figure 8, bottom, and the alignment in Figure 1). This might explain the similar SARs of the *N*<sup>4</sup>-substituent at 5-HT<sub>1A</sub> and D<sub>2</sub> receptors. In contrast, a number of residues in the model that surround the heteroaryl moiety (*i.e.*, Thr160, Trp161, and Gly164, helix IV; Ser199, Thr200, Ala203, and Phe204, helix V; Phe362, Ala365, and Leu366, helix VI) differ from those in D<sub>2</sub> receptors. Observed differences between 5-HT<sub>1A</sub> and D<sub>2</sub> receptors in this region are Thr160 ↔ Val, Gly164 ↔ Ser, Thr200 ↔ Ser, Ala203 ↔ Ser, Ala365 ↔ His, and Leu366 ↔ Ile, respectively (see Figure 8, bottom, and the alignment in Figure 1). This is in good agreement with the SAR data of our compounds, which show that the arylpiperazine part itself is not very well accommodated by the D<sub>2</sub> receptor. In contrast, the 5-HT<sub>1A</sub> receptor can accommodate rather bulky arylpiperazine substituents like the dioxane ring in **27** and **33** and even the additional CH<sub>2</sub>OH group of **1**. In the model, the dioxane ring of these compounds has a close contact with the small and lipophilic Ala365. This residue is replaced with a bulky and polar histidine in D<sub>2</sub> receptors (see Figure 1), which may account for the low tolerance of bulky arylpiperazine substituents at D<sub>2</sub> receptors. Thus, selectivity for 5-HT<sub>1A</sub> versus D<sub>2</sub> receptors is mainly caused by the aryl substitution pattern of the arylpiperazine moiety.

In our model, the CH<sub>2</sub>OH group has no additional interaction with the receptor. This is in agreement with SAR data that show no contribution of this group to 5-HT<sub>1A</sub>-receptor affinity.

## Conclusions

5-HT<sub>1A</sub>-receptor affinity and selectivity versus D<sub>2</sub> receptors of the potent 5-HT<sub>1A</sub> receptor agonist flesinoxan (**1**) and a series of analogous *N*<sup>4</sup>-substituted arylpiperazines were studied. The selectivity of **1** was shown to emerge mainly from the *N*<sup>1</sup>-aryl substitution pattern. For both 5-HT<sub>1A</sub> and D<sub>2</sub> receptors, SARs at the *N*<sup>4</sup>-substituent appeared to be dominated by lipophilicity. Therefore, variation in this part of the structure did not yield selective compounds.

5-HT<sub>1A</sub>-receptor affinities could be rationalized with a computer modeling study. The bioactive conformation was investigated. The results were used to study the interactions of the ligands in a 5-HT<sub>1A</sub>-receptor model that we have previously reported. The coplanar conformation of the arylpiperazine moiety, which was shown to be preferred by *N*<sup>4</sup>-unsubstituted 5-HT<sub>1A</sub>-receptor agonists, can also be adopted by the *N*<sup>4</sup>-substituted agonists **1**, **27**, and **33**. In this conformation, the plane angle between the benzene and piperazine ring is approximately  $30^\circ$ . In the bioactive conformation of the agonists **1**, **27**, and **33**, the *N*<sup>4</sup>-substituent is probably directed *anti*-periplanar with respect to the



**Table 6.** Crystal Structure<sup>a</sup> and Conformations (A–H) Resulting from RANDOMSEARCH Analysis of  $\tau_3$  and  $\tau_4$  of Compound **33** and Subsequent Minimization with MOPAC/AM1

conformation	AM1 energy (kcal/mol)	$\tau_1$ (deg), C6'–C1'–N1–C6	$\tau_2$ (deg), H <sub>N4</sub> –N4–C1''–C2''	$\tau_3$ (deg), N4–C1''–C2''–N3''	$\tau_4$ (deg), C1''–C2''–N3''–C4''
crystal structure	ND	–11.3	176.9	169.7	80.0
A	55.3	–12.8	–178.9	–178.4	66.2
B	55.2	–16.1	–177.5	174.0	–64.3
C	54.2	–16.7	167.9	76.1	–104.2
D	54.2	–14.6	168.2	75.2	–105.9
E	55.2	–14.1	166.1	67.2	65.6
F	56.3	–13.1	170.2	68.1	75.5
G	55.8	–18.3	163.8	64.0	66.9
H	55.2	–16.4	–163.5	–63.8	–63.9

<sup>a</sup> Standard deviations amount 3°, 3°, 2°, and 3° for  $\tau_1$ ,  $\tau_2$ ,  $\tau_3$ , and  $\tau_4$ , respectively.

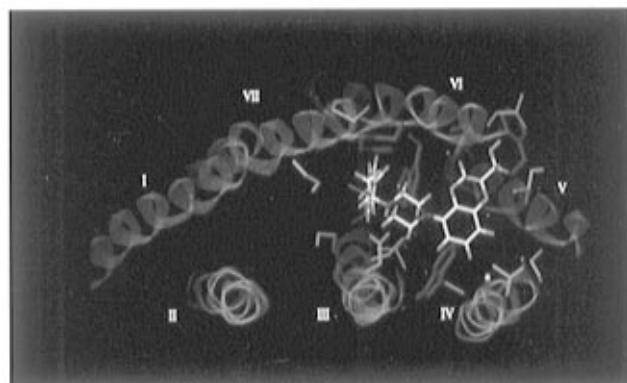
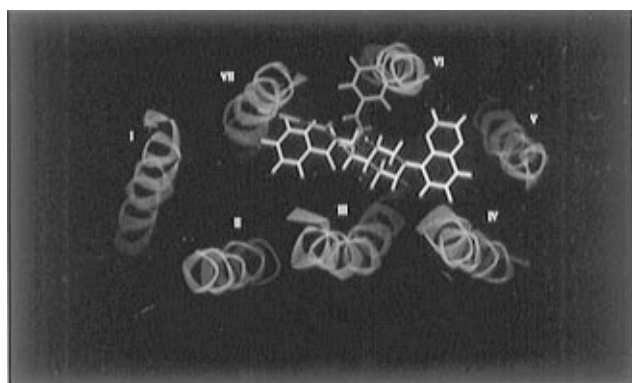


**Figure 7.** (Top) Conformations A (red), B (yellow), and H (blue) of compound **27** in the 5-HT<sub>1A</sub>-receptor model. The overlapping parts of the conformations are white. The *N*<sup>4</sup>-substituents of A and B cause severe steric hindrance with the backbone of helix VII, while the *p*-fluorophenyl substituent of conformation H sticks right through the backbone of helix VI. (Bottom) Position of flesinoxan (**1**) docked into the 5-HT<sub>1A</sub>-receptor model in conformation C and subsequently minimized. The model is viewed from the extracellular side. In contrast to the conformations A, B, and H, the *N*<sup>4</sup>-substituent in conformations C–G is located in the available space between the helices III, VI, and VII.

H<sub>N4</sub> atom. Eight of such *anti*-periplanar conformations (A–H), among which is the crystal structure of **33**, could be identified as potentially bioactive at 5-HT<sub>1A</sub> receptors. Five of these conformations fitted the 5-HT<sub>1A</sub> receptor model well. The predominantly hydrophobic residues of helices III, VI, and VII, which surround the *N*<sup>4</sup>-substituent, are identical for 5-HT<sub>1A</sub> and D<sub>2</sub> receptors. Six of the residues that surround the benzodioxane ring of flesinoxan (**1**) in the 5-HT<sub>1A</sub>-receptor model are different from those in D<sub>2</sub> receptors. Thus, the positions of the 5-HT<sub>1A</sub> agonists **1**, **27**, and **33** in the receptor model, in the potentially bioactive conformations, agree

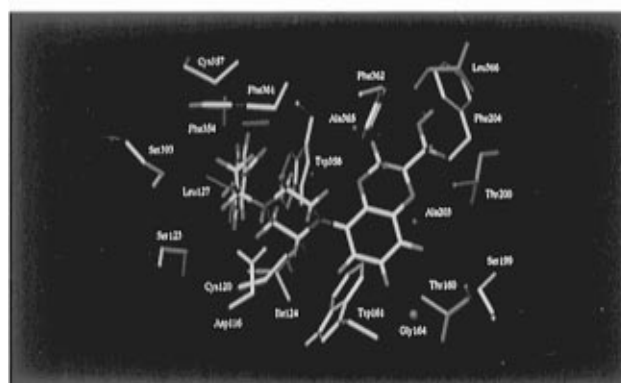
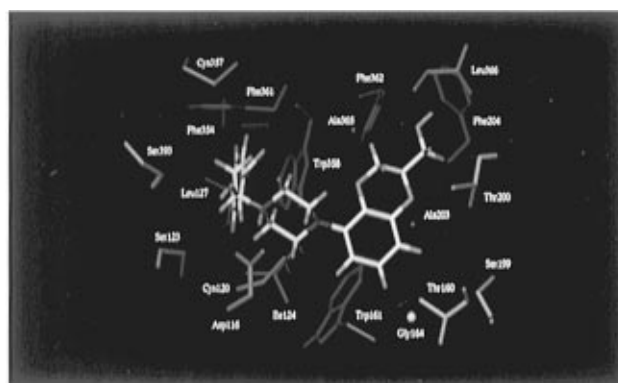


**Figure 8.** More detailed view of the environment of flesinoxan (**1**) docked into the 5-HT<sub>1A</sub>-receptor model in conformation C and subsequently minimized. (Top) The hydrophobic residues Cys120, Ile124, Leu127, and Cys357 (green) and the aromatic residues Phe354, Trp358, and Phe361 (blue) form a lipophilic pocket at one side of the *N*<sup>4</sup>-substituent. At the other side of the pocket two hydrophilic (pink) serine residues are observed (at positions 123 and 393). (Bottom) Residues in the binding pocket that are similar to (yellow) or different from (pink) those in D<sub>2</sub> receptors. All residues that surround the *N*<sup>4</sup>-substituent in the 5-HT<sub>1A</sub>-receptor model are identical with those at similar positions in the D<sub>2</sub> rat receptor, according to the alignment of Figure 1 (*i.e.*, yellow residues Asp116, Cys120, Ser123, Ile124, Leu127, Phe354, Cys357, Trp358, Phe361, and Ser393). Several of the residues that surround the *N*<sup>1</sup>-aryl part are different from those in D<sub>2</sub> receptors (*i.e.*, pink residues Thr160, Gly164, Thr200, Ala203, Ala365, and Leu366).

with 5-HT<sub>1A</sub> SARs and account for the selectivity of flesinoxan (**1**) versus D<sub>2</sub> receptors.

### Experimental Section

**Chemistry.** Melting points are uncorrected. <sup>1</sup>H NMR spectra were recorded on a Bruker WP-200 or AM-400 spectrometer. Chemical shifts ( $\delta$ ) are expressed in parts per million (ppm) relative to internal tetramethylsilane (TMS);

coupling constants ( $J$ ) are in hertz; for clarity the piperazine nitrogen atoms were numbered as in Figure 2. Elemental analyses were performed at the Mikroanalytisches Labor Pascher, Remagen-Bandorf, Germany. Thin-layer chromatography (TLC) was run on Merck silica gel 60 F-254 plates. For normal pressure and flash chromatography, Merck silica gel type 60 (size 70–230 and 230–400 mesh, respectively) was used. Unless stated otherwise, all starting materials were high-grade commercial products. All reactions were performed under a nitrogen atmosphere.

Compounds **28** and **29** are commercially available. Compounds **1**, **26**, and **27** were prepared according to Patent Application EP 0138280,<sup>18</sup> and compounds **8** and **18** were made according to patent application EP 0104614.<sup>19</sup> Compounds **11**, **15**, **20**, and **23–25** were synthesized as described in Patent Applications ES 2027898,<sup>20</sup> JP 60169742,<sup>21</sup> DE 2053759,<sup>22</sup> WO 9109594,<sup>23</sup> FR 1349636,<sup>24</sup> and FR 1537901,<sup>25</sup> respectively. The syntheses of compounds **19** and **30** have been described in refs 26 and 27, respectively. Compounds **31** and **32** were synthesized according to Patent Application JP 61152655.<sup>28</sup>

The *N*-2-(acylamino)ethyl-substituted (2-methoxyphenyl)-piperazines **7**, **9**, **10**, and **12–14** were prepared by acylation of the known *N*-2-aminoethyl precursor **35**,<sup>29</sup> using either the anhydride, the acyl chloride, or the Mukayama ester of the corresponding acids. Compounds **16** and **17** were obtained by the method in Scheme 1 and compounds **21** and **22** by the method in Scheme 2, and compound **33** was obtained according to Scheme 3.

**N**-[2-[4-(2-Methoxyphenyl)-1-piperazinyl]ethyl]acetamide (**7**). A 3.03-g (12.8 mmol) sample of **35** was dissolved in 20 mL of toluene, and a 1.8-mL portion (19 mmol) of acetic anhydride was slowly added during which the temperature increased from 20 to 40 °C. After stirring for 2 h, the solvent was removed *in vacuo*, and the white product was recrystallized from diethyl ether: yield 2.04 g (57%);  $R_f$  0.25 (CH<sub>2</sub>Cl<sub>2</sub>–MeOH, 95:5); mp 96–98 °C; <sup>1</sup>H NMR (CDCl<sub>3</sub>) δ 1.98 (s, 3H, COCH<sub>3</sub>), 2.4–2.8 (cluster, 6H, CH<sub>2</sub> pip and N<sup>4</sup>-CH<sub>2</sub>), 3.09 (m, 4H, CH<sub>2</sub> pip), 3.38 (q, 2H, CONHCH<sub>2</sub>,  $J = 6$ ), 3.84 (s, 3H, OCH<sub>3</sub>), 6.14 (broad peak, 1H, CONH), 6.94 (cluster, 4H, Ph). Anal. (C<sub>15</sub>H<sub>23</sub>N<sub>3</sub>O<sub>2</sub>) C, H, N.

**N**-[2-[4-(2-Methoxyphenyl)-1-piperazinyl]ethyl]-2-thiophenecarboxamide (**9**). A 1.50-g (16 mmol) portion of 2-thiophenecarboxylic acid chloride was prepared from 2-thiophenecarboxylic acid according to a literature procedure.<sup>30</sup> It was dissolved in 10 mL of CH<sub>2</sub>Cl<sub>2</sub> and slowly added to a solution of 2.34 g (18 mmol) of **35** in 10 mL of CH<sub>2</sub>Cl<sub>2</sub>, resulting in an exothermic reaction. After cooling, the white product crystallized from the solvent, was filtered off, and was washed with cold CH<sub>2</sub>Cl<sub>2</sub>: yield 1.50 g (39.5%); mp 207–208 °C (dissolution); <sup>1</sup>H NMR (DMSO–CDCl<sub>3</sub>, 4:1) δ 3.0–3.8 (cluster, 12H, N-CH<sub>2</sub>'s), 3.81 (s, 3H, OCH<sub>3</sub>), 6.9 (cluster, 4H, Ph), 7.14 (dd, 1H, thiophene H-3,  $J = 4$  and 5), 7.71 (dd, 1H, thiophene H-2,  $J = 1$  and 5), 7.94 (dd, 1H, thiophene H-4,  $J = 1$  and 4), 9.03 (t, 1H, CONH,  $J = 6$ ), 10.6 (broad peak, 1H, NH<sup>+</sup>). Anal. (C<sub>18</sub>H<sub>23</sub>N<sub>3</sub>O<sub>2</sub>S·HCl) C, H, N.

**N**-[2-[4-(2-Methoxyphenyl)-1-piperazinyl]ethyl]-2-furan-carboxamide (**10**). A 1.93-g portion of 2-furoic acid chloride (15 mmol) was prepared from 2-furoic acid according to a literature procedure.<sup>30</sup> It was dissolved in 10 mL of CH<sub>2</sub>Cl<sub>2</sub> and slowly added to a solution of 3.5 g (15 mmol) of **35** in 10 mL of CH<sub>2</sub>Cl<sub>2</sub>, during which a precipitate was formed. The reaction mixture was stirred for 12 h at room temperature; the precipitate was filtered off and recrystallized from EtOH: yield 1.95 g (36%); mp 210–211 °C; <sup>1</sup>H NMR (DMSO–CDCl<sub>3</sub>, 4:1) δ 2.9–3.8 (cluster, 12H, N-CH<sub>2</sub>'s), 3.80 (s, 3H, OCH<sub>3</sub>), 6.61 (dd, 1H, furan H-3,  $J = 2$  and 3), 6.9 (cluster, 4H, Ph), 7.18 (dd, 1H, furan H-4,  $J = 1$  and 3), 7.80 (dd, 1H, furan H-2,  $J = 2$  and 1), 8.76 (t, 1H, CONH,  $J = 6$ ), 10.4 (broad peak, 1H, NH<sup>+</sup>). Anal. (C<sub>18</sub>H<sub>23</sub>N<sub>3</sub>O<sub>3</sub>·HCl·0.10H<sub>2</sub>O) C, H, N.

**N**-[2-[4-(2-Methoxyphenyl)-1-piperazinyl]ethyl]-4-pyridinecarboxamide (**12**). The intermediate Mukayama ester of 4-pyridinecarboxylic acid was prepared *in situ* from 1.23 g (10 mmol) of the acid, 3.4 mL (25 mmol) of triethylamine, and 3.2 g (12.5 mmol) of 2-chloro-1-methylpyridinium iodide in 80 mL of CH<sub>2</sub>Cl<sub>2</sub>, according to a literature procedure.<sup>31</sup> The Mukayama reagent was subsequently added to a solution of

2.35 g (10 mmol) of **35** in 40 mL of CH<sub>2</sub>Cl<sub>2</sub>. The reaction mixture was heated at reflux for 2 h, stirred at room temperature for 12 h, acidified with 50 mL of 2 N HCl, and twice extracted with 50 mL of CH<sub>2</sub>Cl<sub>2</sub>. The organic layers were discarded, and the residue was brought at pH > 13 with Na<sub>2</sub>CO<sub>3</sub> and 2 N NaOH followed by three times extraction with 70 mL of CH<sub>2</sub>Cl<sub>2</sub>. The combined organic layers were dried on anhydrous Na<sub>2</sub>SO<sub>4</sub>, filtered once, concentrated *in vacuo*, and purified by silica gel (300 g) column chromatography using CH<sub>2</sub>Cl<sub>2</sub>–MeOH, 90:10: yield 2.2 g. The white HCl salt was obtained by addition of 3 equiv of HCl in 50 mL of EtOH. Recrystallization from EtOH yielded 1.60 g (39%); mp 228–231 °C; <sup>1</sup>H NMR (D<sub>2</sub>O) δ 3.5–3.8 (cluster, 10H, CH<sub>2</sub> pip, N<sup>4</sup>-CH<sub>2</sub>), 3.93 (s, 3H, OCH<sub>3</sub>), 3.98 (t, 2H, CONHCH<sub>2</sub>,  $J = 6$ ), 7.05–7.4 (cluster, 4H, PhOCH<sub>3</sub>), 8.43 (m, 2H, pyridine H-3, H-5), 9.01 (m, 2H, pyridine H-2, H-6). Anal. (C<sub>19</sub>H<sub>24</sub>N<sub>4</sub>O<sub>2</sub>·3HCl·0.25H<sub>2</sub>O) C, H, N.

**N**-[2-[4-(2-Methoxyphenyl)-1-piperazinyl]ethyl]-4-pyrimidinecarboxamide (**13**). A portion of 1.42 g of 4-pyrimidinecarboxylic acid chloride (10 mmol) was prepared from 4-pyrimidinecarboxylic acid according to a literature procedure.<sup>30</sup> It was suspended in 15 mL of CH<sub>2</sub>Cl<sub>2</sub> and added to a solution of 2.35 g (10 mmol) of **35** in 30 mL of CH<sub>2</sub>Cl<sub>2</sub>, resulting in a exothermic reaction. The reaction mixture was stirred for 1 h at room temperature and then filtered over Hyflo. The solvent was evaporated, and the remainder was treated with active coal in an EtOAc–EtOH mixture, recrystallized from EtOH–*i*-PrOH, isolated by filtration, and washed with isopropyl alcohol and diethyl ether: yield 1.61 g (43%); mp 249.5–250.5 °C;  $R_f$  0.5 (CH<sub>2</sub>Cl<sub>2</sub>–MeOH, 90:10); <sup>1</sup>H NMR (DMSO–CDCl<sub>3</sub>, 4:1) δ 3.0–3.9 (cluster, 15H, N-CH<sub>2</sub>'s, OCH<sub>3</sub>), 6.9 (cluster, 4H, Ph), 8.76 (dd, 1H, pyrimidine H-6,  $J = 2$  and 3), 8.89 (d, 1H, pyrimidine H-5,  $J = 3$ ), 9.24 (d, 1H, pyrimidine H-3,  $J = 2$ ), 9.31 (t, 1H, CONH,  $J = 6$ ), 10.6 (broad peak, 1H, NH<sup>+</sup>). Anal. (C<sub>18</sub>H<sub>23</sub>N<sub>5</sub>O<sub>2</sub>·HCl) C, H, N.

**N**-[2-[4-(2-Methoxyphenyl)-1-piperazinyl]ethyl]-3-pyridinecarboxamide (**14**). Compound **14** was synthesized analogous to compound **12**, using 2.35 g (10 mmol) of **35** and a Mukayama reagent of 1.25 g (10 mmol) of 3-pyridinecarboxylic acid, 3.4 mL (25 mmol) of triethylamine, and 3.2 g (12.5 mmol) of 2-chloro-1-methylpyridinium iodide, prepared according to a literature procedure:<sup>31</sup> yield 1.45 g (35%); mp 216–220.5 °C; <sup>1</sup>H NMR (DMSO–CDCl<sub>3</sub>, 4:1) δ 3.2–3.4 (cluster, 4H, CH<sub>ax</sub> pip), 3.45 (t, 2H, N<sup>4</sup>-CH<sub>2</sub>), 3.53 (d, 2H, N<sup>4</sup>-CH<sub>eq</sub> pip), 3.73 (br d, 2H, N<sup>1</sup>-CH<sub>eq</sub> pip), 3.83 (s, 3H, OCH<sub>3</sub>), 3.83 (m, 2H, CONHCH<sub>2</sub>), 6.86–7.08 (m, 4H, Ph), 8.09 (dd, 1H, pyridine H-5,  $J = 6$  and 8), 9.00 (m, 1H, pyridine H-4), 9.03 (m, 1H, pyridine H-6), 9.46 (br s, 1H, pyridine H-2), 9.70 (t, 1H, CONH,  $J = 6$ ). Anal. (C<sub>19</sub>H<sub>24</sub>N<sub>4</sub>O<sub>2</sub>·3HCl) C, H, N.

**N**-[2-[4-(2-Methoxyphenyl)-1-piperazinyl]ethyl]cyclohexanecarboxamide (**16**) (Scheme 1, i). A total of 3.13 g (10 mmol) of **15** and 2.22 g (10 mmol) of P<sub>2</sub>S<sub>5</sub> were suspended in 30 mL of CH<sub>2</sub>Cl<sub>2</sub>. A 5.12-mL volume (40 mmol) of Et<sub>3</sub>N was added while the reaction mixture was stirred and cooled. After 24-h storage at room temperature, the whole was extracted with water. After drying (Na<sub>2</sub>SO<sub>4</sub>), the organic layer was loaded on a dry silica gel (170 g) column and eluted with EtOAc, yielding 1.9 g of a yellow viscous oil (free base). The HCl salt was obtained by addition of 1 equiv of HCl in absolute EtOH and subsequent recrystallization from EtOH–petroleum ether (40–60 °C): yield 1.25 g (35%); mp 151–151.5 °C; <sup>1</sup>H NMR (DMSO–CDCl<sub>3</sub>, 4:1) δ 1.1–1.9 (cluster, 10H, cyclohexyl), 2.68 (broad peak, 1H, cyclohexyl), 3.0–3.8 (cluster, 10H, N-CH<sub>2</sub>'s), 3.80 (s, 3H, OCH<sub>3</sub>), 4.0 (m, 2H, CONHCH<sub>2</sub>), 6.9 (cluster, 4H, Ph), 10.24 (t, 1H, CSNH,  $J = 6$ ), 11.1 (broad peak, 1H, NH<sup>+</sup>). Anal. (C<sub>20</sub>H<sub>31</sub>N<sub>3</sub>O<sub>3</sub>·HCl·0.25H<sub>2</sub>O) C, H, N.

**N**-[2-[4-(2-Methoxyphenyl)-1-piperazinyl]ethyl]cyclohexanecarboximidamide (**17**) (Scheme 1, ii). A 5.7-g portion (30 mmol) of cyclohexanecarboximidic acid ethyl ester was prepared from cyanocyclohexane *via* the method given in Patent Application EP 528633.<sup>33</sup> It was added to a solution of 7.0 g (30 mmol) of **35** in 30 mL of EtOH and kept at room temperature for 5 days. The solvent was removed *in vacuo*, taken up in absolute EtOH, and filtered. The HCl salt was

obtained by addition of 1 equiv of HCl in absolute EtOH and subsequent recrystallization from absolute EtOH: yield 6.7 g (59%); mp >258 °C (dissolution); <sup>1</sup>H NMR (DMSO-CDCl<sub>3</sub>, 4:1) δ 1.1–1.9 (cluster, 10H, cyclohexyl), 2.6 (broad peak, 1H, cyclohexyl), 3.1–3.9 (cluster, 12H, N-CH<sub>2</sub>'s), 3.82 (s, 3H, OCH<sub>3</sub>), 6.9 (cluster, 4H, Ph), 9.20 (broad peak, 1H, imino protonated), 9.31 (broad peak, 1H, imino protonated), 9.82 (t, 1H, CONH, *J* = 6), 11.4 (broad peak, 1H, NH<sup>+</sup>). Anal. (C<sub>20</sub>H<sub>32</sub>N<sub>4</sub>O·2HCl·0.5H<sub>2</sub>O) C, H, N.

**1-[4-(4-Fluorophenyl)-1-but-3-enyl]-4-(2-methoxyphenyl)piperazine (22) (Scheme 2, i, ii).** The intermediate compound 4-(4-fluorophenyl)-3-buten-1-ol (**36**) was synthesized according to a literature procedure.<sup>34</sup> To a solution of 2 g (12 mmol) of **36** and 5 mL (34 mmol) of Et<sub>3</sub>N in 100 mL of CH<sub>2</sub>Cl<sub>2</sub> at -20 °C (CO<sub>2</sub>/acetone) was added 5 mL of methanesulfonyl chloride (26 mmol) while stirring. The reaction mixture was stirred at 0 °C for 30 min and then for 12 h at room temperature, poured into 100 mL of 1 N HCl, and extracted twice with 100 mL of CH<sub>2</sub>Cl<sub>2</sub>. The combined organic layers were dried (Na<sub>2</sub>SO<sub>4</sub>), and the solvent was removed *in vacuo*, yielding 3.17 g of a light-brown oil.

The oil was dissolved in 100 mL of acetonitrile, and 2.26 mL of diisopropylethylamine (13 mmol) was added followed by a 2.28-mL portion of *N*-(2-methoxyphenyl)piperazine (13 mmol). The reaction mixture was stirred for 12 h at 60 °C. The solvent was removed, and the residue was taken up in EtOAc and extracted with 200 mL of 2 N NaOH and 100 mL of saturated NaCl solution, respectively. The organic layer was dried (Na<sub>2</sub>SO<sub>4</sub>), the solvent was removed *in vacuo*, and the residue was purified over 300 mL of silica gel using EtOAc as eluent. Solvent evaporation of the combined fractions yielded 2.6 g of light-yellow oil (free base of compound **22**).

A 1.25-g portion (3.7 mmol) of this oil was dissolved in 15 mL of EtOAc, and a solution of 0.43 g (3.7 mmol) of fumaric acid in 2.5 mL of absolute EtOH was added. The solvent was removed, and the residue was stirred in diisopropyl ether, collected by filtration, and washed with diisopropyl ether and petroleum ether. The obtained white solid was dried *in vacuo* at 38 °C above KOH: yield 1.38 g (82%); mp 165–167 °C (dissolution); <sup>1</sup>H NMR (DMSO-CDCl<sub>3</sub>, 4:1) δ 2.44 (m, 2H, H=CHCH<sub>2</sub>), 2.63 (m, 2H, N<sup>4</sup>-CH<sub>2</sub>'s), 2.70 (m, 4H, N<sup>4</sup>-CH<sub>2</sub> pip), 3.04 (m, 2H, N<sup>1</sup>-CH<sub>2</sub> pip), 3.80 (s, 3H, OCH<sub>3</sub>), 6.21 (dt, 1H, H=CHCH<sub>2</sub>, *J* = 7, 13 and 16), 6.44 (broad peak, 1H, Ph-CH=CH, *J* = 16), 6.62 (s, 2H, fum), 6.85–7.0 (cluster, 4H, PhOCH<sub>3</sub>), 7.06 (m, 2H, *p*-F-Ph *meta* H's), 7.38 (m, 2H, *p*-F-Ph *ortho* H's). Anal. (C<sub>21</sub>H<sub>25</sub>FN<sub>2</sub>O·C<sub>4</sub>H<sub>4</sub>O<sub>4</sub>) C, H, N.

**1-[4-(4-Fluorophenyl)-1-butyl]-4-(2-methoxyphenyl)piperazine (21) (Scheme 2, iii).** A 1.37-g portion (4 mmol) of **22** was dissolved in 100 mL of EtOH with 0.5 g of 10% Pd on C catalyst and hydrogenated at room temperature for 2 h. The catalyst was removed by filtration over Hyflo followed by rinsing with EtOH. The solvent of the filtrate was removed *in vacuo* yielding 1.2 g of a light-yellow oil (free base of compound **21**). This was taken up in 25 mL of EtOAc and a solution of 0.41 g of fumaric acid (3.5 mmol) in 4 mL of absolute EtOH was added during which a white precipitate was formed. This was stirred at room temperature for 1 h and then collected and washed with EtOH, diisopropyl ether, and petroleum ether. Drying *in vacuo* at 38 °C above KOH yielded 1.36 g of **21** (74%); mp 170–171 °C (dissolution); <sup>1</sup>H NMR (DMSO-CDCl<sub>3</sub>, 4:1) δ 1.48–1.66 (cluster, 4H, NCH<sub>2</sub>CH<sub>2</sub>CH<sub>2</sub>), 2.51 (t, 2H, PhCH<sub>2</sub>), 2.60 (t, 2H, N<sup>4</sup>-CH<sub>2</sub>), 2.67 (m, 4H, N<sup>4</sup>-CH<sub>2</sub> pip), 3.02 (m, 4H, N<sup>1</sup>-CH<sub>2</sub> pip), 3.79 (s, 3H, OCH<sub>3</sub>), 6.61 (s, 2H, fum), 6.83–6.98 (cluster, 4H, PhOCH<sub>3</sub>), 7.02 (m, 2H, *p*-F-Ph *meta* H's), 7.20 (m, 2H, *p*-F-Ph *ortho* H's). Anal. (C<sub>21</sub>H<sub>27</sub>FN<sub>2</sub>O·C<sub>4</sub>H<sub>4</sub>O<sub>4</sub>) C, H, N.

***N*-[2-(1-Methoxy-1-oxopropyl)]-*N*-(phenylmethyl)alanine Methyl Ester (38) (Scheme 3, i).** *N*-(Phenylmethyl)-D-alanine methyl ester (**37**)<sup>35</sup> and 3-[[trifluoromethyl)sulfonyl]oxy]propanoic acid methyl ester<sup>13</sup> were synthesized according to published procedures. A 229.7-g portion (0.97 mol) of racemic 3-[[trifluoromethyl)sulfonyl]oxy]propanoic acid methyl ester was mixed with 177 mL of diisopropylethylamine. While cooling, a 163.4-g (0.845 mol) portion of **37** was slowly added, resulting in a very exothermic reaction and producing a viscous precipitate. Consequently, the reaction mixture

could not be stirred. The mixture was heated at 90 °C overnight. After cooling, 1.5 L of *n*-pentane was added, and the precipitate was removed using suction filtration and washed three times with large volumes of *n*-pentane. The solvent of the filtrate was evaporated *in vacuo* at 50 °C yielding 235.1 g of a mixture of the *meso* and *d,l* forms of **38** (99.5%) as light-brown crystals.

***N*-(1-Carboxyethyl)-*N*-(phenylmethyl)alanine (39) (Scheme 3, ii).** A 139.65-g portion (0.5 mol) of **38** was dissolved in 585 mL of MeOH, and a solution of 96.2 g of 87.5% KOH (1.5 mol) in 300 mL of water was added. This mixture was stirred and heated at reflux for 4.5 h. After cooling the reaction mixture was concentrated to ca. 250 mL using rotary evaporation and filtered over Hyflo. The filtrate was heated on a steam bath to prevent crystallization of the dipotassium salt, and 125 mL of 12 N HCl was added in portions. At the last portion the desired product started crystallizing, and the gray solid was collected at room temperature. The crude product was recrystallized by concentrating a solution in 4.5 L of absolute EtOH to ca. 1.75 L on a steam bath. After cooling the product was collected, washed with diethyl ether, and dried *in vacuo* yielding 97.9 g of **39** (77.9%).

**1-(2,3-Dihydro-1,4-benzodioxin-5-yl)-3,5-dimethyl-4-(phenylmethyl)-2,6-piperazinedione (40) (Scheme 3, iii).** Compound **40** was synthesized from 7.8 g (31 mmol) of **39**, 4.7 g (31 mmol) of 5-aminobenzo-1,4-dioxane, and 5 g (31 mmol) of *N,N'*-carbonyldiimidazole in THF according to a literature procedure:<sup>14</sup> yield 6.7 g (59%).

**1-(2,3-Dihydro-1,4-benzodioxin-5-yl)-3,5-dimethylpiperazine (41, 42) (Scheme 3, iv, v).** A mixture of compounds **41** and **42** was obtained *via* hydrogenation of 18.3 mmol of **40** followed by reaction with 2.8 equiv of borane–methyl sulfide complex in THF and 6 N HCl, similar to a procedure described before.<sup>14</sup> The *cis*- and *trans*-isomers **41** and **42** were separated using flash chromatography (CH<sub>2</sub>Cl<sub>2</sub>–MeOH–ammonia, 97:2.5:0.5), giving 1.7 g of **41**, 2.6 g of **42**, and 1.4 g of a *cis/trans*-mixture: total yield 5.7 g (63%).

***N*-[2-[4-(2,3-Dihydro-1,4-benzodioxin-5-yl)-*cis*-2,6-dimethyl-1-piperazinyl]ethyl]-4-fluorobenzenecarboxamide (33) (Scheme 3, vi).** A 1.7-g sample (6.85 mmol) of the *cis*-isomer **41** was dissolved in 50 mL of acetone, and 1.29 g (7.7 mmol) of *N*-(4-fluorobenzoyl)aziridine (obtained *via* a literature procedure)<sup>36</sup> was added. The solvent was removed *in vacuo* from the reaction mixture using rotary evaporation, yielding a light-brown solid. The fumarate was obtained by dissolving the solid in 20 mL of absolute EtOH and addition of 1 equiv of fumaric acid in 10 mL of absolute EtOH followed by concentration to ca. 10 mL (rotary evaporation). A 75-mL volume of diethyl ether was added, and the desired compound started crystallizing after scratching the laboratory glass. The product was collected as white crystals, washed with diethyl ether, and air-dried: yield 1.0 g (28%); mp 213–217 °C; <sup>1</sup>H NMR (DMSO-CDCl<sub>3</sub>, 4:1) δ 1.14 (d, 6H, -CH<sub>3</sub>, *J* = 6), 2.32 (t, 2H, N<sup>1</sup>-CH<sub>ax</sub> pip, *J* = 10), 2.8 (cluster, 4H, N<sup>4</sup>-CH<sub>2</sub>'s), 3.25 (broad peak, 2H, N<sup>1</sup>-CH<sub>eq</sub> pip, *J* = 10), 3.34 (m, 2H, CON-HCH<sub>2</sub>), 4.22 (m, 4H, Bzd CH<sub>2</sub>'s), 6.42 (dd, 1H, Bzd *ortho* H, *J* = 2 and 8), 6.48 (dd, 1H, Bzd *para* H, *J* = 2 and 8), 6.62 (s, 2H, fum), 6.69 (t, 1H, Bzd *meta* H, *J* = 8), 7.25 (m, 2H, *p*-F-Ph *meta* H's), 7.9 (m, 2H, *p*-F-Ph *ortho* H's), 8.55 (t, 1H, CONH, *J* = 6). Anal. (C<sub>23</sub>H<sub>28</sub>FN<sub>3</sub>O<sub>3</sub>·0.5C<sub>4</sub>H<sub>4</sub>O<sub>4</sub>·0.5H<sub>2</sub>O) C, H, N.

**log *P* Determination.** Partition coefficients (*n*-octanol/water) were measured by a high-performance liquid chromatographic (HPLC) method based on an OECD (Organisation for Economic Co-operation and Development) method,<sup>37</sup> using a mobile phase buffered at pH > 11 and an aluminum-based octadecyl-modified stationary phase. The measured retention factor *k* of a compound was correlated with its partition coefficient using a calibration graph based on 10 reference compounds with well-known log *P*<sub>ow</sub> values in the range 2.1–5.7.

**Crystal Structure Determination and Refinement of 33.** Determination was carried out (monoclinic, space group *P*<sub>2</sub><sub>1</sub>/*c* (No. 14) with *a* = 10.4183(6), *b* = 10.7524(5), and *c* = 21.656(2) Å; β = 107.218(5)°, *V* = 2317.2(2) Å<sup>3</sup>; *Z* = 4, *R*<sub>1</sub> = 0.0595, ω*R*<sub>2</sub> = 0.1438, *S* = 1.04). A colorless, plate-shaped crystal was cut to size and glued to the tip of a Lindemann

glass capillary and transferred to an Enraf-Nonius CAD4-T diffractometer equipped with a rotating anode. Unit-cell parameters and an orientation matrix were determined by least-squares refinement of 25 well-centered reflections (SET4)<sup>38</sup> in the range  $10.0^\circ < \Theta < 14.0^\circ$ . Reduced-cell calculations did not indicate higher lattice symmetry.<sup>39</sup> All data were collected in  $\omega$  scan mode. Data were corrected for Lp effects and the observed linear decay of 2% of the three periodically measured reference reflections. The structure was solved by automated direct methods (SHELXS86).<sup>40</sup> Refinement on  $F^2$  was carried out by full-matrix least-squares techniques (SHELXL-93);<sup>41</sup> no observance criterion was applied during refinement. All non-hydrogen atoms were calculated and refined with anisotropic thermal parameters. The hydrogen atoms were refined with a fixed isotropic thermal parameter amounting to 1.5 or 1.2 times the value of the equivalent isotropic thermal parameter of their carrier atoms, for the hydrogen atoms on the methyl groups and the other hydrogen atoms, respectively. The hydrogens on N were refined without constraints. Weights were introduced in the final refinement cycles. Crystal data and details on data collection and refinement, as well as final positional parameters, can be obtained as Supporting Information. Neutral atom scattering factors and anomalous dispersion corrections were taken from *International Tables for Crystallography*.<sup>42</sup> Geometrical calculations and illustrations were performed with PLATON.<sup>43</sup> All calculations were performed on a DEC station 5000/125.

**Modeling. 1. Software and Hardware.** Small-ligand building, docking procedures, and all computations (MAXIMIN, MOPAC) were performed with the SYBYL package, version 6.1a (Tripos Associates, Inc., St. Louis, MO), running on a Silicon Graphics Iris Indigo Elan 4000. For MAXIMIN calculations (Tripos force field), the Powell method was chosen (default values).

**2. Ligand Building and Minimizations.** The geometry of the crystal structure of compound **33** was used as a basis for modeling the other ligands. All phenylpiperazines were built by modification of this structure with the SKECTCH option in SYBYL. For the study of the first torsion angle  $\tau_2$  with MOPAC (AM1, CHARGE=1, PRECISE),<sup>16</sup> the structures of compounds **43** and **44** (Figure 3) were minimized over all bonds and angles, except the torsion angle  $\tau_2$ , which was constrained at values between  $0^\circ$  and  $360^\circ$  ( $10^\circ$  intervals). The crystal structure coordinates of **33** were also used in the RANDOMSEARCH option of the SYBYL program for the study of  $\tau_3$  and  $\tau_4$  (default values were used; a chirality check was applied; energy cutoff was at 120 kcal/mol; the arylpiperazine moiety was constrained by defining it as an *aggregate*). It was previously shown that MOPAC/AM1 is more suitable for full energy minimization of arylpiperazine structures than molecular mechanics (MM) calculations (*e.g.*, Tripos force field).<sup>15</sup> Therefore, structures that emerged from the RANDOMSEARCH analysis were further minimized with MOPAC/AM1 (default values; additional keywords MMOK, PRECISE, and CHARGE=1). Only low-energy conformations (energy less than 3 kcal/mol above the absolute minimum energy) were investigated further.

**3. Model Building and Docking.** A model of the 5-HT<sub>1A</sub> receptor was built according to Kuipers *et al.*<sup>11,12</sup> The position of eltoprazine (**31**) in the receptor model, which is described in ref 11, was taken as a starting point. The compounds **1**, **27**, and **33** were docked into the receptor model in conformations A–H, by fitting them on (docked) compound **31**. The relative orientation with respect to **31** was derived by a straightforward fit of the arylpiperazine parts. Two atoms in the phenyl ring (C3' and C5'), the basic nitrogen atom, and its proton were used as fitting points. Subsequently, eltoprazine (**31**) was removed from the model. Conformations C–G could fit the model without causing severe hindrance with backbone atoms. The complexes of each compound **1**, **27**, and **33** in conformations C–G with the receptor were energy-minimized using molecular mechanics calculations. For this purpose, an "active site" was created, containing all side chains of residues within a distance of 4 Å from the ligand (see Figure 8). These side chains, and the ligand itself, were allowed to optimize their position and conformation; the backbone atoms

were kept fixed. The Tripos force field tends to underestimate the conjugation of the nitrogen lone pair with the aromatic ring system. Therefore, the torsion angle  $\tau_1$  was constrained at the current values as calculated by MOPAC/AM1 (force constant was 100 kcal/(mol deg<sup>2</sup>)). The distance between the Asp116 oxygen atoms and the H<sub>N4</sub> atom was constrained at 2.0 Å (force constant was 100 kcal/(mol Å<sup>2</sup>)).

**Biochemistry. 1. Receptor Binding Assay.** Radioligand binding studies were carried out using [<sup>3</sup>H]-2-(di-*n*-propylamino)-8-hydroxytetralin (8-OH-DPAT)<sup>44</sup> and [<sup>3</sup>H]-8-[3-(*p*-fluorobenzoyl)propyl]-1-phenyl-1,3,8-triazaspiro[4.5]decan-4-one (spiperone)<sup>45</sup> as radioligands on rat frontal cortex and rat corpus striatum, respectively.

**2. In Vitro Functional Assay.** CHO cells, stably expressing human 5-HT<sub>1A</sub> receptors, were obtained from Allelix Biopharmaceuticals Inc., Ontario, Canada.

Cells were cultured in  $\alpha$ -DMEM (Dulbecco's Modified Eagle's Medium) containing 10% fetal calf serum. Three days prior to experimentation, cells were seeded in 24-well plates with a density of  $0.5 \times 10^5$  cells/well. Assessment of adenylate cyclase activity was done essentially according to Weiss *et al.*<sup>46</sup> Cells were incubated with [<sup>3</sup>H]adenine (NEN; 2  $\mu$ Ci/mL) in  $\alpha$ -DMEM for 2 h. Subsequently, cells were rinsed once with PBS containing 10 mM IBMX, after which cells were stimulated for 10 min in PBS/IBMX with forskolin ( $10^{-7}$  M) in the presence of compounds at various concentrations, determined in quadruplicate. Cells were extracted with 5% TCA, containing excess nonradioactive ATP and cAMP. [<sup>3</sup>H]cAMP and [<sup>3</sup>H]-ATP were separated by sequential chromatography over Dowex 50-WX4 and aluminum oxide according to Salomon *et al.*,<sup>47</sup> and eluates were analyzed for radioactivity by liquid scintillation counting.

5-HT<sub>1A</sub>-receptor-mediated inhibition of forskolin-stimulated accumulation of cAMP was analyzed by a four-parameter logistic regression function, using the nonlinear curve-fitting program INPLOT (ISI Software, Philadelphia, PA). EC<sub>50</sub> values of three independent experiments were obtained and are presented as mean value  $\pm$  SEM.

**Acknowledgment.** We wish to thank Erik Ronken and Annemarije Menkveld of the Pharmacology Department, CNS Cell Biology, for determination of the functional properties of compounds **27** and **33**. We thank Piet Hoogkamer and Gemma Feenstra-Bielders for the experimental determination of log *P* values. We also thank Rolf Feenstra, Paul van Vliet (IRI, Delft, The Netherlands), and Koos Tipker for helpful discussions and Petra Lelieveld and Netty Rengelink for their substantial secretarial support.

**Supporting Information Available:** Crystal data and details on data collection and crystal structure determination, including final positional parameters, atomic coordinates for the hydrogen atoms, bond lengths and angles, thermal parameters, and a thermal motion ellipsoid plot for **33** (8 pages). Listings of observed and calculated structure factor amplitudes for **33** (13 pages). Ordering information is given on any current masthead page.

## References

- (1) Saudou, F.; Hen, R. 5-Hydroxytryptamine Receptor Subtypes in Vertebrates and Invertebrates. *Neurochem. Int.* **1994**, *25*, 503–532.
- (2) Peroutka, S. J. Serotonin Receptor Subtypes. Their Evolution and Clinical Relevance. *CNS Drugs* **1995**, *4* (Suppl. 1), 18–28.
- (3) Middlemiss, D. N.; Fozard, J. R. 8-Hydroxy-2-(di-*n*-propylamino)-tetralin Discriminates between Subtypes of the 5-HT<sub>1</sub> Recognition Site. *Eur. J. Pharmacol.* **1983**, *90*, 151–153.
- (4) van Wijngaarden, I.; Tulp, M. Th. M.; Soudijn, W. The Concept of Selectivity in 5-HT Receptor Research. *Eur. J. Pharmacol.-Mol. Pharmacol. Sect.* **1990**, *188*, 301–312.
- (5) Björk, L.; Cornfield, L. J.; Nelson, D. L.; Hillver, S. E.; Anden, N. E.; Lewander, T. Pharmacology of the Novel 5-Hydroxytryptamine Receptor Antagonist (S)-5-Fluoro-8-Hydroxy-2-(Dipropylamino) Tetralin: Inhibition of (R)-8-Hydroxy-2-(Dipropylamino) Tetralin-Induced Effects. *J. Pharmacol. Exp. Ther.* **1991**, *258*, 58–65.

- (6) Cliffe, I. A.; Brightwell, C. I.; Fletcher, A.; Forster, E. A.; Mansell, H. L.; Mansell, Y. R.; Routledge, C.; White, A. C. (*S*)-*N*-tert-Butyl-3-(4-(2-methoxyphenyl)piperazin-1-yl)-2-phenylpropanamide [(*S*)-WAY-100135]: A Selective Antagonist at Presynaptic and Postsynaptic 5-HT<sub>1A</sub> Receptors. *J. Med. Chem.* **1993**, *36*, 1509–1510.
- (7) Glennon, R. A.; Naiman, N. A.; Lyon, R. A.; Titeler, M. Arylpiperazine Derivatives as High-Affinity 5-HT<sub>1A</sub> Serotonin Ligands. *J. Med. Chem.* **1988**, *31*, 1968–1971.
- (8) For examples, see: (a) Abou-Gharbia, M.; Patel, U. R.; Webb, M. B.; Moyer, J. A.; Andree, T. H.; Muth, E. A. Polycyclic Aryl and Heteroaryl piperazinyl Imides as 5-HT<sub>1A</sub> Receptor Ligands and Potential Anxiolytic Agents: Synthesis and Structure-Activity Relationship Studies. *J. Med. Chem.* **1988**, *31*, 1382–1392. (b) Scott, M. K.; Martin, G. E.; DiStefano, D. L.; Fedde, C. L.; Kubkla, M. J.; Barrett, D. L.; Baldy, W. J.; Elgin, R. J., Jr.; Kesslick, J. M.; Mathiasen, J. R.; Shank, R. P.; Vaught, J. R. Pyrrole Mannich Bases as Potential Antipsychotic Agents. *J. Med. Chem.* **1992**, *35*, 552–558. (c) Peglion, J.; Canton, H.; Bervoets, K.; Audinot, V.; Brocco, M.; Gobert, A.; Le Marouille-Girardon, S.; Millan, M. J. Characterization of Potent and Selective Antagonists at Postsynaptic 5-HT<sub>1A</sub> Receptors in a Series of N4-Substituted Arylpiperazines. *J. Med. Chem.* **1995**, *38*, 4044–4055.
- (9) Mokrosz, J. L.; Pietrasiewicz, M.; Duszynska, B.; Cegla, M. T. Structure Activity Relationship Studies of Central Nervous System Agents. 5. Effect of the Hydrocarbon Chain on the Affinity of 4-Substituted 1-(3-chlorophenyl)piperazines for 5-HT<sub>1A</sub> Receptor Site. *J. Med. Chem.* **1992**, *35*, 2369–2374.
- (10) van Steen, B. J.; van Wijngaarden, I.; Tulp, M. Th. M.; Soudijn, W. Structure-Affinity Relationship Studies on 5-HT<sub>1A</sub> Receptor Ligands. 1. Heterobicyclic Phenylpiperazines with N4-Alkyl Substituents. *J. Med. Chem.* **1993**, *36*, 2751–2760.
- (11) Kuipers, W.; van Wijngaarden, I.; Kruse, C. G.; ter Horst-van Amstel, M.; Tulp, M. Th. M.; IJzerman, A. P. N<sup>4</sup>-unsubstituted N<sup>1</sup>-Arylpiperazines as High-Affinity 5-HT<sub>1A</sub> Receptor Ligands. *J. Med. Chem.* **1995**, *38*, 1942–1954.
- (12) Kuipers, W.; van Wijngaarden, I.; IJzerman, A. P. A Model of the Serotonin 5-HT<sub>1A</sub> Receptor: Agonist and Antagonist Binding Sites. *Drug Des. Discovery* **1994**, *11*, 231–249.
- (13) Effenberger, F.; Burkard, U.; Willfahrt, J. Trifluoromethanesulfonates of  $\alpha$ -Hydroxycarboxylates - Educts for the Racemization - Free Synthesis of N-substituted  $\alpha$ -Amino Acids. *Angew. Chem., Int. Ed. Engl.* **1983**, *22*, 65.
- (14) Kruse, C. G.; Troost, J. J.; Cohen-Fernandes, P.; van der Linden, H.; van Loon, J. D. Single-Step Conversion of Aliphatic, Aromatic, and Heteroaromatic Primary Amines into Piperazine-2,6-diones. *Recl. Trav. Chim. Pays-Bas* **1988**, *107*, 303–309.
- (15) Dijkstra, G. D. H. Conformational Analysis of 1-Arylpiperazines and 4-Arylpiperidines. *Recl. Trav. Chim. Pays-Bas* **1993**, *112*, 151–160.
- (16) Stewart, J. J. P. MOPAC: A Semiempirical Molecular Orbital Program. *J. Comput. Aided Mol. Des.* **1990**, *4*, 1–105.
- (17) van Steen, B. J.; van Wijngaarden, I.; Tulp, M. Th. M.; Soudijn, W. Structure-Affinity Relationship Studies on 5-HT<sub>1A</sub> Receptor Ligands. 2. Heterobicyclic Phenylpiperazines with N4-Aralkyl Substituents. *J. Med. Chem.* **1994**, *37*, 2761–2773.
- (18) Blood-Pressure Lowering Piperazine Derivatives. Patent Application EP0138280; *Chem. Abstr.* **1985**, *103*, 123520.
- (19) Phenylpiperazine Derivatives. Patent Application EP0104614; *Chem. Abstr.* **1984**, *101*, 110952.
- (20) Process for Preparation of New (2-Methoxyphenyl)piperazine Derivatives with 5-HT<sub>1A</sub> Receptor Activity. Patent Application ES2027898; *Chem. Abstr.* **1992**, *118*, 124560.
- (21) Phenylpiperazine Derivatives. Patent Application JP60169472; *Chem. Abstr.* **1985**, *104*, 109689.
- (22) 1-Hydroxy- and 1-Oxo-1-phenyl- (or Heteroaryl)-4-(1-piperazinyl)butanes. Patent Application DE2053759; *Chem. Abstr.* **1971**, *75*, 49136.
- (23) Preparation of Substituted Phenylisopropylamines and Analogs as Sigma Receptor Ligands for Treatment of Schizophrenia and Psychoses. Patent Application WO9109594; *Chem. Abstr.* **1991**, *115*, 182801.
- (24) Nouveaux Derives de la Piperazine, Utilisables en Therapeutique. Patent Application FR1349636; *World Patent Index* **1966**, 10820F.
- (25) *N*-(4-Phenyl-1-Piperazinyl)alkyl Halo (and Nitro) Benzamides. Patent Application FR1537901; *Chem. Abstr.* **1969**, *71*, 70637.
- (26) Soudijn, W.; van Wijngaarden, I.; Allewijn, F. T. N. Distribution, Excretion and Metabolism of Neuroleptics of the Butyrophenone Type. I. Excretion and Metabolism of Haloperidol and Nine Related Butyrophenone Derivatives in Wistar Rats. *Eur. J. Pharmacol.* **1967**, *1*, 47–57.
- (27) Van Wijngaarden, I.; Kruse, C. G.; van der Heyden, J. A. M.; Tulp, M. Th. M. 2-Phenylpyrroles as Conformationally Restricted Benzamide Analogues. A New Class of Potential Antipsychotics. 2. *J. Med. Chem.* **1988**, *31*, 1934–1940.
- (28) Preparation of Piperazines as Psychotropics. Patent Application JP61152655; *Chem. Abstr.* **1986**, *106*, 5080.
- (29) Mull, R. P.; Mizzoni, R. H.; Dapero, M. R.; Egbert, M. E. Guanidines with Antihypertensive Activity. II. *J. Med. Pharm. Chem.* **1962**, *5*, 944.
- (30) Barcock, R.; Chadwick, D.; Storr, R.; Fuller, L.; Young, J. Synthesis of Some Novel Imidate Derivatives of Thiophene and Furan: Investigations of Their Methylation Properties and Some Synthetic Applications. *Tetrahedron* **1994**, *50*, 4149.
- (31) Degani, Y.; Heller, A. Direct Electrical Communication Between Chemically Modified Enzymes and Metal Electrodes. 2. Methods for Bonding Electron-Transfer Relays to Glucose Oxidase and D-Amino-Acid Oxidase. *J. Am. Chem. Soc.* **1988**, *110*, 2615.
- (32) Feng, Z.; Gollamudi, R.; Purcell, W.; Hill, R.; Korfmacher, W. Molecular Determinants of the Platelet Aggregation Inhibitory Activity of Carbamoylpiperidines. *J. Med. Chem.* **1992**, *35*, 2952.
- (33) Preparation of *N*-(Oxoalkyl)-5-(Acylamino)-6-Oxopyrimidin-1-ylacetamides as Elastase Inhibitors. Patent Application EP0528633; *Chem. Abstr.* **1993**, *119*, 72617.
- (34) Cheik-Rouhou, F.; Le Bigot, Y.; El Gharbi, R.; Delmas, M.; Gaset, A. A Simplified Wittig Synthesis Using a Solid-Liquid Transfer Process: VI. Synthesis of  $\gamma$ -Unsaturated Alcohols from Aromatic and Heteroaromatic Aldehydes. *Synth. Commun.* **1986**, *16*, 1617.
- (35) Kubota, H.; Kubo, A.; Takahashi, H.; Shimizu, R.; Date, T.; Okamura, K.; Nunami, K. Stereospecific Amination by Dynamic Kinetic Resolution Utilizing 2-Oxoimidazolidine-4-carboxylate as a Novel Chiral Auxiliary. *J. Org. Chem.* **1995**, *60*, 6776.
- (36) Pettit, G.; Gupta, S.; Whitehouse, P. Antineoplastic Agents XVIII. *N*-(2-Haloethyl)benzylamines. *J. Med. Chem.* **1967**, *10*, 692–696.
- (37) OECD Guideline for Testing of Chemicals No. 117, adopted at Mar. 30, 1989.
- (38) de Boer, J. L.; Duisenberg, A. J. M. Diffractometer Software (CAD4F). *Acta Crystallogr.* **1984**, *A40*, C410.
- (39) Spek, A. L. LEPAGE - An MS-DOS Program for the Determination of the Metrical Symmetry of a Translation Lattice. *J. Appl. Crystallogr.* **1988**, *21*, 578–579.
- (40) Sheldrick, G. M. *SHELXS86 Program for Crystal Structure Determination*; University of Göttingen: Göttingen, Germany, 1986.
- (41) Sheldrick, G. M. *SHELXL-93 Program for Crystal Structure Refinement*; University of Göttingen: Göttingen, Germany, 1993.
- (42) Wilson, A. J. C., Ed. *International Tables for Crystallography*; Kluwer Academic Publishers: Dordrecht, The Netherlands, 1992; Vol. C.
- (43) Spek, A. L. PLATON, An Integrated Tool for the Analysis of the Results of Single Crystal Structure Determination. *Acta Crystallogr.* **1990**, *A46*, C34.
- (44) Gozlan, H.; El Mestikawy, S.; Pichet, L.; Glowinsky, J.; Hamon, M. Identification of Presynaptic Serotonin Autoreceptors Using a New Ligand: [<sup>3</sup>H]-PAT. *Nature* **1983**, *305*, 140–142.
- (45) Creese, I.; Schneider, R.; Snyder, S. H. [<sup>3</sup>H]Spiroperidol Labels Dopamine Receptors in Pituitary and Brain. *Eur. J. Pharmacol.* **1977**, *46*, 377–381.
- (46) Weiss, S.; Sebben, M.; Bockaert, J. Corticotropin-Peptide Regulation of Intracellular Cyclic AMP Production in Cortical Neurons in Primary Culture. *J. Neurochem.* **1985**, *45*, 869–874.
- (47) Salomon, Y.; Londos, C.; Rodbell, M. A Highly Sensitive Adenylate Cyclase Assay. *Anal. Biochem.* **1974**, *58*, 541–548.
- (48) Sequences were obtained from the SWISSPROT database, A. Bairoch, Dept. Biochimie Medicinale, Centre Medicinal Universitaire, 1211 Geneva 4, Switzerland, and SWISS-PROT Protein sequence database, EMBL Data Library, D-69117 Heidelberg, Germany.
- (49) Spek, A. L. *PLUTON Molecular Graphics Program*; Utrecht University: Utrecht, The Netherlands, 1995.

JM9604960